Michael Buchwitz on behalf of all co-authors 21-August-2018

Authors response to referee comments on revised version of manuscript "Computation and analysis of atmospheric carbon dioxide annual mean growth rates from satellite observations during 2003-2016" of Michael Buchwitz et al., MS No.: acp-2018-158

Dear Editor,

many thanks for giving us the opportunity to respond to the referees comments and concerns and to submit a revised version of our manuscript.

Unfortunately, we have not been able to convince the referees with our initial answers and our initial revised version of our manuscript although we tried as good and carefully as possible to address all concerns.

Both referees still insist on major modifications. Because of this and because the new comments provide a better understanding on our side what exactly the concerns are, we now provide a significantly improved version of our manuscript addressing the two remaining referee comments (please see our detailed "Point-by-point response to the referees comments and concerns" below).

Implementation of the recommended changes resulted in significant modifications of our manuscript as shown below in the "List of all relevant changes" and in the "Marked-up manuscript version" attached at the end of this document.

We hope that this revised version of the manuscript is acceptable for you and for the reviewers and that it meets the high standards of ACP.

Michael Buchwitz

on behalf of all co-authors

The following pages contain the following information:

- List of all relevant changes
- Point-by-point response to the referees comments and concerns
- The marked-up manuscript version

List of all relevant changes:

Both reviewers criticize that we also present growth rates for latitude bands. To address this we have implemented the following modifications:

- We have removed all references to this from the abstract, from the main part and from the Conclusions section.
- Instead we have added a new Annex A where we show our results for the latitude bands (for the reason why we have not entirely removed this please see our detailed answer to the referees comments).
- The Annex contains a new figure (Fig. A2) which shows a comparison of our growth rate uncertainties with the difference between two NOAA annual mean growth rate time series (Mauna Loa – Global) to support that "we expect similar annual mean CO_2 growth rates, i.e., agreement within measurement error, for the different latitude bands and globally". We have added this in response to the referees concern.
- As a consequence of this the corresponding figure (now Fig. A1) and table (now Tab. A1) has been been moved from the main part to the Annex and one figure has been removed.
- The figure now shown as Fig. 3 has been improved by adding error bars to the time series shown in Fig. 3a.

Both reviewers also provide critical comments related to our growth rate variance analysis. To address this we are now

- providing in Sect. 4 an additional introduction paragraph which includes and explicit formulation of the question we are answering (in Sect. 4), how we answer it and what our main assumptions are. We have added this to address the concern that is was not clear "what we are doing and why" and what the "new knowledge" is (note that in our point-by-point response to the referees comments we now also provide a list of what we consider the most relevant "new knowledge" provided by our paper). In this context, we have also added two additional references (Betts et al., 2016, and Kim et al., 2016). We hope that all is much clearer now by explicitly formulating a question (which we think is an important one) and the corresponding answer obtained using a transparent and well-explained method.

Furthermore, we have implemented minor text changes at various places to further improve the manuscript.

Reply to Anonymous Referee #1 comments on revised manuscript

In the following, we provide answers to each of the referee's comments and concerns.

General:

Referee C1:
My two main criticisms of this paper were their use of: 1) regional atmospheric growth rates and 2) a simple statistical model to attribute changes in atmospheric CO_2 to human emissions and ENSO. Neither comment is addressed well by the authors.

Author's reply:
In our reply to your initial comments and concerns, we aimed at providing clear and appropriate answers and modified our manuscript accordingly. Too bad that we failed to explain our arguments good enough and/or that our arguments do not convince you. We try to do better this time and have also implemented major manuscript modifications. Please see below our feedback to your remaining / new comments. Based on your comments we have generated another (second) revised version of our manuscript.

Results for latitude bands:

Referee C2:
Their response to my first comment is limited to two additional statements neither of which I fully understand: a) "Growth rate time series for several latitude bands are shown in Fig. 4. As can be seen from Fig. 4, the growth rates are similar in all latitude bands including the global results (for numerical values see Tab. 2). The reason for this is that atmospheric CO_2 is long-lived and therefore well-mixed." b) "As a result of atmospheric transport and mixing, similar mean annual CO_2 growth rates, within their measurements error, are expected for all values derived at the different latitude bands. This behaviour is shown in Fig. 4 and is interpreted as an indication of the good quality of the satellite XCO_2 data product and the adequacy of the method used to compute the annual mean CO_2 growth rates." Atmospheric CO_2 is well mixed but the authors are trying to determine the small, annual changes that sit on the growing well-mixed background. Atmospheric CO_2 has an interhemispheric gradient, which is determined by hemispheric differences in emissions but also by the ~1 year mean interhemispheric crossing time. It can take weeks-months for signals to be transported from the tropics to midlatitudes so a seasonal change in one latitude band in year one may straddle growth rates in that year and year two. I also don't follow their argument about using regional growth rates to comment on the quality of the CO_2 data.

Author's reply:
In our response to your earlier comments on this topic, we tried to explain in detail why we have applied our method also to latitude bands (and not only to the global data set). Thanks to your new comment (shown above) we now understand your concern better.

In our manuscript, we focus on the gobal results (comparison with NOAA growth rates, time series correlation analysis with emissions and ENSO indices) but we think that it is important to also show results for latitude bands. As explained, we expect similar growth rates for all latitude bands and we show that this is what we find. Our findings therefore agree with our assumptions (our knowledge) and we interpret this (as written in our manuscript) as a confirmation of the good quality of the satellite data and of the method to derive growth rates from these data as we do not get "strange" growth rates for certain latitude bands which would indicate a potential problem.

Unfortunately, we neither managed to convince you nor the other referee. Therefore, we now decided to remove all results related to latitude bands from the abstract, from the main part and from the Conclusions section but to show the results related to latitude bands instead in a new dedicated Annex A. We also discussed to entirely remove all results related to latitude bands from the manuscript but for the reasons explained (see above and below) we think that these are important results that should be shown in the paper and we think that moving this into an Annex is a good compromise. We are now also better addressing your concerns as stated in your comment by adding an additional figure, which shows an estimate of the expected latitudinal difference (for details see below).

This results in text modifications at various places including the Abstract, main text and Conclusions section and it results in (i) moving Fig. 4 and Tab. 2 to the new Annex A, (ii) the removal of Fig. 2 and (iii) adding a new Figure A2.

Here the text we plan to show in the new Annex A:

“Growth rate time series have also been computed for several latitude bands as shown in Fig. A1. As can be seen, the growth rates agree within their 1-sigma uncertainty range in all latitude bands including the global results (for numerical values see Tab. A1).
The reason for this is that atmospheric CO_2 is long-lived and therefore well-mixed. Because of this we expect similar annual mean CO_2 growth rates, i.e., agreement within measurement error, for the different latitude bands and globally. Identical growth rates are not expected due to differences in the sources and sinks and the time needed for transport and mixing. The expectation of similar growth rates is corroborated by Fig. A2, which shows a comparison of the uncertainty of the satellite-derived growth rates (red bars) with the difference of two annual mean CO_2 growth rate time series from NOAA, namely the time series from Mauna Loa, Hawaii, and the global time series obtained from globally averaged marine surface data (both obtained from https://www.esrl.noaa.gov/gmd/ccgg/trends/gr.html). As shown in Fig. A2, the uncertainty of the satellite data is similar (mean value: 0.34 ppm/year) as the difference between the two NOAA time series (standard deviation: 0.21 ppm/year). We acknowledge that the maximum difference between any two latitude bands may be somewhat larger than the difference between the two NOAA time series shown in Fig. A2, but it is assumed that the difference shown in Fig. A2 is at least a reasonable approximation.
The agreement shown in Fig. A1 is interpreted as an indication of the good quality of the satellite XCO_2 data product and of the adequacy of the method used to compute the annual mean CO_2 growth rates because we do not find “strange values” in certain latitude bands or certain years, which would be an indication for a potential problem.”

Time series variance analysis:

Referee C3:
Their response to my second comment is a bit odd in my opinion. I agree that attempting to attribute observed changes in atmospheric CO2 to human emissions and ENSO is of great importance. However, my original comment said that the method they used to attribute human emissions and ENSO was a fool's errand. I made this comment for a number of reasons:
* the spatial and temporal distributions of human emissions and the manifold responses of the land biosphere to regional weather patterns are not necessarily distinct.
* is there a disprovable result reported by this correlation analysis? The approach/results are so amorphous and ill defined that I find it hard to understand what new knowledge I have gained from this analysis.
* if, as the authors claim, their analysis are not in conflict with Liu et al then they should show it.

Author's reply:

Concerning "spatial and temporal distributions of human emissions and land biosphere responses": They may not be perfectly distinct but we assume that they are to a large degree distinct. After all most human emissions from fossil fuel burning do not take place where, for example, most of the land biosphere is located. The spatial distribution should not be a major issue for our analysis as we focus on global averages (and for latitude bands please see above). Concerning temporal distributions and land biosphere responses we address this (at least to some extent) by our time lag analysis and our time lag analysis results agree well with previous research as shown in our manuscript. Furthermore, we also take the temporal correlation between human emissions and the (time shifted) ENSO indices into account.

Concerning "Is there a disprovable result reported by this correlation analysis?":
We have formulated all our conclusions carefully in order not to claim something that is not supported by our analysis. Our main conclusion is (see Conclusions section): "This analysis shows that the ENSO impact on CO_2 growth rate variations dominates over that of human emissions throughout the period 2003-2016 but in particular in the second half of this period, i.e., during 2010-2016". This is a disprovable result as, in principle, someone may show that this is wrong. In our analysis, we assume that the growth rate variation in the investigated time period is dominated by human emissions and ENSO. We furthermore assume that ENSO is well described by the used ENSO indices. If these assumptions are not valid, then our conclusions may be wrong. However, we also consider the uncertainties we are reporting. Therefore, in more quantitative terms, we conclude: "We estimate the probability that the impact of ENSO on the variability is larger than the impact of human emissions to be 63% for the time period 2003-2016. If the time period is restricted to 2010-2016 this probability increases to 94%". These statements are based on Monte Carlo simulations taking into account the uncertainties of the growth rates. The percentages show that we are quite sure that our findings are robust for the period 2010-2016 but that we are less sure for the period 2003-2016.
In the new revised version we will explain more explicitly what our main assumption are by adding this new paragraph at the beginning of Sect. 4: 'It is well known that changes of the growth rate of atmospheric CO_2 have anthropogenic and natural causes (e.g., Jones et al., 2001; Betts et al., 2016; Kim et al., 2016; Liu et al., 2017; Chylek et al., 2018). In this section we are aiming at answering the following question: "Assuming that the variability of the CO_2 growth rate is dominated by ENSO and by human emissions, which of the two considered causes dominates the growth rate variability given the satellite-derived growth rates and their uncertainty?". To answer this question we are using a simple linear statistical model and time series of human emissions and two ENSO indices assuming that these indices are appropriate proxies for ENSO related effects in the context of providing a reliable answer.'. Concerning "new knowledge" please see the list we provide at the end of our response.

This paragraph contains two additional references, which we added to our manuscript:

Betts et al., 2016: Betts, R. A., Jones, C. D., Knight, J. R., Keeling, R. F., and Kennedy, J. J., El Niño and a record CO_2 rise, Nature Climate Change, vol. 6, 806–810, https://www.nature.com/articles/nclimate3063.pdf , 2016.

Kim et al., 2016: Kim, J.-S., Kug, J.-S., Yoon, J.-H., Jeong, S.-J., Increased Atmospheric CO_2 Growth Rate during El Niño Driven by Reduced Terrestrial Productivity in the CMIP5 ESMs, Journal of Climate, 8783-8805, 29. 10.1175/JCLI-D-14-00672.1, 2016.

Concerning “amorphous and ill defined”:
We disagree that our approach is “amorphous and ill defined”. The opposite is true: We use a very simple and well-defined method based on well established other data sets (published and publicly available annual CO_2 emissions and time series of ENSO indices) and we explain everything clearly so that it can be easily reproduced by others. We agree, however, that the problem is a complex one. Here we aim at answering only one specific question (as already explained above, this question is now given explicitly in our manuscript at the beginning of Sect. 4): “Assuming that the variability of the CO_2 growth rate is dominated by ENSO and by human emissions, which of the two considered causes is the dominating one given the satellite-derived growth rates and their uncertainty?” We clearly explained this method and its results (i.e., the answer to the question) and this is new knowledge presented in our manuscript (for the complete list of “new knowledge” please see below). So we answered one question (which we think is an interesting one) but we were not aiming at answering all questions related the impact of ENSO and anthropogenic emissions on CO_2 growth rates.

Concerning Liu et al:
In our paper we cite the Liu et al., 2017, Science paper only in the context of the discussion of the large 2015/2016 growth rates: “As can also be seen from Fig. 2c, the largest growth rates are approximately 3 ppm/year during 2015 and 2016. These record large growth rates (Peters et al., 2017) are attributed to the consequences of the strong 2015/2016 El Niño event, which produced large CO_2 emissions from fires and enhanced net biospheric respiration in the tropics relative to normal conditions (Heymann et al., 2017; Liu et al., 2017)”. In our paper, we do not claim anything that goes beyond this. We only refer to the Liu et al. and Heymann et al. papers as they provide relevant information in the context of the discussion of the growth rates. In particular we have not identified anything that points to a (potential) conflict.

However, in our response to your initial comments we wrote: “The interesting work of Liu et al 2017 (Science) uses a complex earth model, constrained by a limited number of satellite observations in the tropics and other a priori knowledge, to identify different responses in the different tropical continents to the surface flux of CO_2 and thus carbon. Our approach to quantify the different roles of ENSO and anthropogenic fossil fuel emissions uses the reported time series of mean annual CO_2 growth rates and well-established time series of ENSO indices and the known estimates of anthropogenic emissions from fossil fuel combustion and industry. This approach is our attempt to address what we and others consider an important issue viz: the attribution of growth rate variations to known anthropogenic emissions from fossil fuel combustion and industry and to that from the impact of ENSO. The latter has many potential impacts on the earth system amongst which are in the tropics the creation of regions of flooding and drought, increasing fire and biomass burning and changing sea surface temperature. These effects all impact on the growth rate of CO_2 in different ways. However, in this study we have not tried to separate the different impacts of ENSO. Rather in this study, we attribute the importance of ENSO and the known anthropogenic fossil fuel combustion and industry sources to the observed annual growth rates. Our results are not in conflict with the scientific finding of Liu et al 2017 (Science). The use of our longer term time series of XCO_2 provides an opportunity when coupled with models to investigate the regional impacts of ENSO both in the tropics and the extra tropics in a separate study. Overall, we consider that our approach is relevant, reasonable and plausible. We describe our assumptions and the derivation of the attribution clearly so that readers can reproduce the results, criticise our assumptions and make improved analyses.”. This answer contains the sentence “Our results are not in conflict with the scientific finding of Liu et al 2017 (Science).” We have written this because of the explanation as given above. But perhaps this sentence is too strong / misleading. What we mean is that we have not identified any aspect where we are in conflict with the findings of Liu et al. (and nothing in this direction is mentioned in our manuscript). We should have explained this better in our response to your initial comments and we apologize for not having formulated this clear enough.

Concerning "new knowledge":
In our manuscript, we present the following new knowledge:

- We present a new global total column CO_2 ("XCO_2") data set (based on satellite data) covering 14 years
- We present a new method to compute annual mean XCO_2 growth rates from this data set
- We present a new annual mean CO_2 growth rate time series (covering the entire atmosphere, not only near-surface CO_2) including a comparison with growth rates from NOAA based on surface CO_2 observations; we find agreement within the reported uncertainty ranges and therefore consider our growth rates to be validated
- We present an answer to the question "Assuming that the variability of the CO_2 growth rate is dominated by ENSO and by human emissions, which of the two considered causes dominates the growth rate variability given the satellite-derived growth rates and their uncertainty?" To answer this question we used a statistical analysis method, which we clearly explain. Our answer is given in the Conclusions section: "Our analysis also shows that the ENSO impact on CO_2 growth rate variations dominates over that of human emissions throughout the period 2003-2016 (14 years) but in particular during the period 2010-2016 (second half of the investigated time period) due to strong La Niña and El Niño events. We estimate the probability that the impact of ENSO on the variability is larger than the impact of human emissions to be 63% for the time period 2003-2016. If the time period is restricted to 2010-2016 this probability increases to 94%."

Reply to Anonymous Referee #2 comments on revised manuscript

In the following, we provide answers to each of the referee's comments and concerns. Based on these comments we have generated another (second) revised version of our manuscript.

Referee C1:
The authors have responded to most of my technical comments carefully.

Author's reply:
This is good to know. In fact, we tried to address all comments as good and carefully as possible.

Referee C2:
However, I do not see that they changed much scientifically. E.g., both referees pointed out that a zonal partitioning of the growth rate has little meaning for CO2, yet it's still there, this time with a small disclaimer.

Author's reply:
Unfortunately, you are not referring to our detailed justification as provided in our response to your initial review and why our explanations do not convince you.

In our manuscript, we focus on the gobal results (comparison with NOAA growth rates, time series correlation analysis with emissions and ENSO indices) but we think that it is important to also show results for latitude bands. As explained, we expect similar growth rates for all latitude bands and we show that this is what we find. Our findings therefore agree with our assumptions (our knowledge) and we interpret this (as written in our manuscript) as a confirmation of the good quality of the satellite data and of the method to derive growth rates from these data as we do not get "strange" growth rates for certain latitude bands which would indicate a potential problem.

Unfortunately, we neither managed to convince you nor the other referee. Therefore, we now decided to remove all results related to latitude bands from the abstract, from the main part and from the Conclusions section but to show the results related to latitude bands instead in a new dedicated Annex A. We also discussed to entirely remove all results related to latitude bands from the manuscript but for the reasons explained (see above and below) we think that these are important results that should be shown in the paper and we decide that moving this into an Annex would be a good compromise. We are now also better addressing your concerns as stated in your comment by adding an additional figure, which shows an estimate of the expected latitudinal difference (for details see below).

This results in text modifications at various places including the Abstract, main text and Conclusions section and it results in (i) moving Fig. 4 and Tab. 2 to the new Annex A, (ii) the removal of Fig. 2 and (iii) adding a new Figure A2.

Here the text we plan to show in the new Annex A:

"Growth rate time series have also been computed for several latitude bands as shown in Fig. A1. As can be seen, the growth rates agree within their 1-sigma uncertainty range in all latitude bands including the global results (for numerical values see Tab. A1).
The reason for this is that atmospheric CO_2 is long-lived and therefore well-mixed. Because of this we expect similar annual mean CO_2 growth rates, i.e., agreement within measurement error, for the different latitude bands and globally. Identical growth rates are not expected due to differences in the sources and sinks and the time needed for transport and mixing. The expectation of similar growth rates is corroborated by Fig. A2, which shows a comparison of the uncertainty of the satellite-derived growth rates (red bars) with the difference of two annual mean CO_2 growth rate time series from NOAA, namely the time series from Mauna Loa, Hawaii, and the global time series obtained from globally averaged

marine surface data (both obtained from https://www.esrl.noaa.gov/gmd/ccgg/trends/gr.html). As shown in Fig. A2, the uncertainty of the satellite data is similar (mean value: 0.34 ppm/year) as the difference between the two NOAA time series (standard deviation: 0.21 ppm/year). We acknowledge that the maximum difference between any two latitude bands may be somewhat larger than the difference between the two NOAA time series shown in Fig. A2, but it is assumed that the difference shown in Fig. A2 is at least a reasonable approximation.
The agreement shown in Fig. A1 is interpreted as an indication of the good quality of the satellite XCO_2 data product and of the adequacy of the method used to compute the annual mean CO_2 growth rates because we do not find "strange values" in certain latitude bands or certain years, which would be an indication for a potential problem."

Referee C3:
Moreover, I remain unconvinced that the work is significant enough to qualify for a standalone ACP publication. Typically the analysis presented in this paper would be a small part of a larger paper, say a paper on a source-sink inversion of SCIAMACHY XCO2 or the validation of the XCO2 retrieval algorithm. However, a quantification of the global growth rate (zonal bands, as I said, mean very little) and a comparison to NOAA's MBL growth rate, in my opinion, does not qualify as a solid standalone publication. On this point, I am afraid, the authors and I may never agree.

Author's reply:
As already explained on our detailed response to your initial comments, we do not agree with this. As explained, we think that our manuscript is appropriate for ACP because of the topic and because of the new results, we are presenting.

In our manuscript, we present the following new knowledge:
In our manuscript, we present the following new knowledge:

- We present a new global total column CO_2 ("XCO_2") data set (based on satellite data) covering 14 years
- We present a new method to compute annual mean XCO_2 growth rates from this data set
- We present a new annual mean CO_2 growth rate time series (covering the entire atmosphere, not only near-surface CO_2) including a comparison with growth rates from NOAA based on surface CO_2 observations; we find agreement within the reported uncertainty ranges and therefore consider our growth rates to be validated
- We present an answer to the question "Assuming that the variability of the CO_2 growth rate is dominated by ENSO and by human emissions, which of the two considered causes dominates the growth rate variability given the satellite-derived growth rates and their uncertainty?" To answer this question we used a statistical analysis method, which we clearly explain. Our answer is given in the Conclusions section: "Our analysis also shows that the ENSO impact on CO_2 growth rate variations dominates over that of human emissions throughout the period 2003-2016 (14 years) but in particular during the period 2010-2016 (second half of the investigated time period) due to strong La Niña and El Niño events. We estimate the probability that the impact of ENSO on the variability is larger than the impact of human emissions to be 63% for the time period 2003-2016. If the time period is restricted to 2010-2016 this probability increases to 94%."

The following pages show the

marked-up manuscript version

Computation and analysis of atmospheric carbon dioxide annual mean growth rates from satellite observations during 2003-2016

Michael Buchwitz[1], Maximilian Reuter[1], Oliver Schneising[1], Stefan Noël[1], Bettina Gier[1,2], Heinrich Bovensmann[1], John P. Burrows[1], Hartmut Boesch[3,4], Jasdeep Anand[3,4], Robert J. Parker[3,4], Peter Somkuti[3,4], Rob G. Detmers[5], Otto P. Hasekamp[5], Ilse Aben[5], André Butz[2,6], Akihiko Kuze[7], Hiroshi Suto[7], Yukio Yoshida[8], David Crisp[9], Christopher O'Dell[10]

[1]Institute of Environmental Physics (IUP), University of Bremen, Bremen, Germany

[2]Deutsches Zentrum für Luft- und Raumfahrt e.V. (DLR), Institut für Physik der Atmosphäre, Oberpfaffenhofen, Germany

[3]Earth Observation Science, University of Leicester, Leicester, UK

[4]NERC National Centre for Earth Observation, Leicester, UK

[5]SRON Netherlands Institute for Space Research, Utrecht, The Netherlands

[6]Meteorologisches Institut, Ludwig-Maximilians-Universität (LMU), Munich, Germany

[7]Japan Aerospace Exploration Agency (JAXA), Tsukuba, Japan

[8]National Institute for Environmental Studies (NIES), Tsukuba, Japan

[9]Jet Propulsion Laboratory (JPL), Pasadena, CA, USA

[10]Colorado State University (CSU), Fort Collins, CO, USA

Correspondence to: Michael Buchwitz (Michael.Buchwitz@iup.physik.uni-bremen.de)

Abstract. The growth rate of atmospheric carbon dioxide (CO_2) reflects the net effect of emissions and uptake resulting from anthropogenic and natural carbon sources and sinks. Annual mean CO_2 growth rates have been determined ~~globally and for selected latitude bands~~ from satellite retrievals of column-average dry-air mole fractions of CO_2, i.e., XCO_2, for the years 2003 to 2016. The ~~global~~ XCO_2 growth rates agree with National Oceanic and Atmospheric Administration (NOAA) growth rates from CO_2 surface observations within the uncertainty of the satellite-derived growth rates (mean difference ± standard deviation: 0.0±0.3 ppm/year; R: 0.82). This new and independent data set confirms record large growth rates around 3 ppm/year in 2015 and 2016, which are attributed to the 2015/2016 El Niño. Based on a comparison of the satellite-derived growth rates with human CO_2 emissions from fossil fuel combustion and with El Niño Southern Oscillation (ENSO) indices, we estimate by how much the impact of ENSO dominates the impact of fossil fuel burning related emissions in explaining the variance of the atmospheric CO_2 growth rate.

1 Introduction

Atmospheric carbon dioxide (CO_2) is an important greenhouse gas that causes global warming (IPCC 2013). Sources that emit CO_2 into the atmosphere include anthropogenic and natural sources at the surface, and the oxidation of carbon monoxide and hydrocarbons in the atmosphere. The sinks that remove CO_2 primarily at the surface include biological (photosynthesis) and physical (solubility) processes. Anthropogenic emissions of CO_2, primarily from fossil fuel combustion, have increased the atmospheric CO_2 mixing ratios at the surface by more than 40% since pre-industrial times, from less than 280 parts per million (ppm) to 402.8±0.1 ppm in 2016 (Dlugokencky and Tans, 2017a). A global increase of atmospheric CO_2 by 1 ppm in a one-year time period corresponds to an annual increase of 2.12 GtC/year (Ballantyne et al., 2012). However, this increase in mass does not directly correspond to the emissions. The reason is that only a fraction of the emitted CO_2 remains in the atmosphere as CO_2 is partitioned between the atmosphere and ocean and land carbon sinks. On average, somewhat less than half of the emitted CO_2 remains in the atmosphere but this "airborne fraction" varies substantially from year to year (Le Quéré et al., 2016, 2018). Variations of the airborne fraction are not well understood primarily because of an inadequate understanding of the terrestrial carbon sink, which introduces large uncertainties for climate prediction (e.g., IPCC 2013; Peylin et al., 2013; Wieder et al., 2015; Huntzinger et al., 2017). Identification of the origin of changes of the growth rate requires additional information for the attribution to particular sources or sinks (Peters et al., 2017). Atmospheric CO_2 growth rates inferred from in-situ CO_2 surface measurements are regularly determined and published, for example, by the National Oceanic and Atmospheric Administration (NOAA) (see https://www.esrl.noaa.gov/gmd/ccgg/trends/gr.html). In this study, we present and interpret atmospheric growth rates determined from the remote sensing of CO_2 vertical columns from space, which are described in the following section.

2 Global satellite observations of atmospheric CO_2 columns

Satellites provide retrievals of CO_2 vertical columns in terms of the CO_2 column-average dry-air mole fraction, denoted XCO_2. Although a relatively new field, satellite-based XCO_2 data products have already been used to improve our knowledge of natural (e.g., Basu et al., 2013; Maksyutov et al., 2013; Chevallier et al., 2014; Reuter et al., 2014a; Schneising et al., 2014; Houweling et al., 2014; Parker et al., 2016; Heymann et al., 2017; Liu et al., 2017; Kaminski et al., 2017) and anthropogenic (e.g., Schneising et al., 2013; Reuter et al., 2014b; Kort et al., 2012; Hakkarainen et al., 2016; Nassar et al., 2017) CO_2 sources and sinks but only a few studies explicitly present and discuss CO_2 growth rates. Buchwitz et al., 2007, analyzed the first three years (2003-2005) of XCO_2 retrievals from SCIAMACHY/ENVISAT (Burrows et al., 1995; Bovensmann et al., 1999) generated using the WFM-DOAS retrieval algorithm (Buchwitz et al., 2006). They computed year-to-year CO_2 variations and compared the XCO_2 increase with the XCO_2 increase computed from the output of NOAA's CO_2 assimilating system CarbonTracker (Peters et al., 2007) and found agreement within 1 ppm/year. Schneising et al., 2014, computed growth rates from the 2003-2011 SCIAMACHY XCO_2 record. They compared the derived annual growth rates with surface temperature and found that years having higher temperatures during the vegetation growing season are associated with larger growth rates in atmospheric CO_2 at northern mid-latitudes. Growth rates from GOSAT (Kuze et al., 2016) are published by the National Institute for Environmental Studies (NIES), Tsukuba, Japan (NIES 2017).

In this study, we analyze a new satellite XCO_2 data set covering 14 years (2003-2016) generated from SCIAMACHY/ENVISAT and TANSO-FTS/GOSAT. We use the XCO_2 data product Obs4MIPs (Observations for Model Intercomparisons Project) version 3 (O4Mv3), which is a gridded (Level 3) monthly data product at 5° latitude by 5° longitude spatial resolution in Obs4MIPs format (Buchwitz et al., 2017a). Obs4MIPs (https://www.earthsystemcog.org/projects/obs4mips/) is an activity to make observational products more accessible for climate model intercomparisons (e.g., Lauer et al., 2017). The O4Mv3 XCO_2 data product was generated by gridding (averaging) the XCO_2 Level 2 (i.e., individual soundings) product generated with the Ensemble Median Algorithm (EMMA, Reuter et al., 2013). EMMA uses as input an ensemble of XCO_2 Level 2 data products (Buchwitz et al., 2015, 2017a, 2017b; Reuter et al., 2013) from SCIAMACHY/ENVISAT and TANSO-FTS/GOSAT. To generate the O4Mv3 product, the EMMA version 3.0 (EMMAv3, Reuter et al., 2017e) product was used. The list of satellite products used for the generation of the EMMAv3 Level 2 product - and therefore also for the O4Mv3 Level 3 data product used in this study - is provided in Tab. 1. The quality of this product relative to Total Carbon Column Observing Network (TCCON) ground-based observations (Wunch et al., 2011, 2015) can be summarized as follows (Buchwitz et al., 2017c): +0.23 ppm overall (global) bias, relative accuracy 0.3 ppm (1-sigma), and very good stability in terms of linear bias trend (-0.02±0.04 ppm/year).

Figure 1 presents an overview of the O4Mv3 product in terms of time series and global XCO_2 maps. The maps show the typical coverage of XCO_2 from SCIAMACHY (until April 2012) and GOSAT (since mid 2009). As can be seen, the time series for the three latitude bands shown in Fig. 1 have very similar slopes. They mainly differ in the amplitude of the seasonal cycle, which reflects the latitudinal dependence of uptake and release of atmospheric CO_2 by the terrestrial biosphere (Schneising et al., 2014). These time series have been used to compute annual mean CO_2 growth rates as will be explained in the following section.

3 Atmospheric CO_2 growth rates from satellite observations

National Oceanic and Atmospheric Administration (NOAA) defines the annual mean CO_2 growth rate for a given year as the CO_2 concentration difference at the end of that year minus the CO_2 concentration at the beginning of that year (Thoning et al., 1989; see also additional explanations as given on the NOAA/ESRL website (https://www.esrl.noaa.gov/gmd/ccgg/about/global_means.html)). We adopt this definition. As described below, our method involves the following three steps: (i) Computation of an XCO_2 time series (at monthly resolution and sampling) by averaging the XCO_2 in the region of interest. (ii) Computation of monthly sampled XCO_2 annual growth rates by computing the difference of the XCO_2 value of month i minus the XCO_2 value of month i-12 and computation of the corresponding uncertainty estimate. (iii) Computation of annual mean growth rates and their corresponding uncertainties from the monthly sampled annual growth rates.

In the following, this method is described in detail using Fig. 2 for illustration. ~~Figure 2 shows how the growth rates are computed for the latitude band 30°N-60°N, i.e., for northern mid-latitudes.~~ In Figure 2a monthly satellite XCO_2 (O4Mv3), as obtained by globally averaging all the individual (5°x5°) XCO_2 values ~~in the selected latitude~~

~~band~~, is plotted. To compute the spatially averaged XCO_2 time series (shown in Fig. 2a), we first longitudinally average the XCO_2 followed by the computation of the area-weighted latitudinal average of XCO_2 by using the cosine of latitude as weight. We consider surface area because surface fluxes are linked to mass of CO_2 (or number of CO_2 molecules) rather than molecular mixing ratios or mole fractions. As can be seen, the computed time series does not start at the beginning of 2003 but in April 2003. As explained in Buchwitz et al., 2017d (see discussion of their Fig. 6.1.1.1) the underlying SCIAMACHY BESD v02.01.02 XCO_2 data product (see Tab. 1) apparently suffers from an approximately 1 ppm high bias in the first few months of 2003. The exact magnitude of this bias has not been quantified due to lack of TCCON validation data in this early time period. As this bias in early 2003 is critical for the year 2003 growth rate, we have omitted the first three months of 2003 for the computation of the growth rates shown in this publication.

Figure 2b shows monthly sampled annual growth rates as computed from the monthly XCO_2 values shown in Fig. 2a. Each value is the difference of two monthly XCO_2 values corresponding to the same month (e.g., January) but different years (e.g., 2004 and 2005). For example, the first data point (first diamond symbol) shown in Fig. 2b is the difference of the April 2004 XCO_2 value minus the April 2003 XCO_2 value. The second data point corresponds to May 2004 minus May 2003, etc. The time difference between the monthly XCO_2 pairs is always one year and the time assigned to each XCO_2 difference is the time in the middle of that year. Therefore, the time series shown in Fig. 2b starts six months later and ends six months earlier as compared to the time series shown in Fig. 2a. Each XCO_2 difference shown in Fig. 2b therefore corresponds to an estimate of the XCO_2 annual growth rate and the position on the time-axis corresponds to the middle of the corresponding one-year time period.

A 1-sigma uncertainty estimate has been computed for each of the monthly sampled annual growth rates shown in Fig. 2b (see grey vertical bars). They have been computed such that they reflect the following aspects: (i) the standard error of the O4Mv3 XCO_2 values as given in the O4Mv3 data product file for each of the 5^ox5^o grid cells, (ii) the spatial variability of the XCO_2 within the selected region, (iii) the temporal variability of the annual growth rates in the one year time interval, which corresponds to the annual growth rate, and (iv) the number of months (N) with data located in that one year time interval. The uncertainties have been computed as the mean value of three terms divided by the square root of N. The first term is the mean value of the standard error, the second term is the standard deviation of the XCO_2 values in the selected region and the third term is the standard deviation of the monthly sampled annual growth rates in the corresponding one-year time interval.

Figure 2c shows the final result, i.e., the annual mean XCO_2 growth rates and their estimated (1-sigma) uncertainties. The annual mean growth rates have been computed by averaging all the monthly sampled annual growth rates (shown in Fig. 2b), which are located in the year of interest (e.g., 2003). For most years, 12 annual growth rate values are available for averaging but there are some exceptions. For example, for the year 2003 only 3 values are present as can be seen from Fig. 2b and for the years 2014 and 2015 there are only 11 values as no data are available for January 2015 due to issues with the GOSAT satellite. The uncertainty of the annual mean growth rate has been computed by averaging the uncertainties assigned to each of the monthly sampled annual growth rates (shown as grey vertical bars in Fig. 2b) scaled with a factor, which depends on the number of months (N) available for averaging. This factor is the square root of 12/N. It ensures that the uncertainty is larger, the less data points are available for averaging. Overall, our uncertainty estimate is quite conservative, as we do not assume that errors improve upon averaging. As a result of this procedure, the error bar of the year 2003 growth rate is quite large (0.~~72~~76 ppm/year, see Tab. ~~2~~A1 in Annex A, where all numerical values are listed). This is because the monthly sampled annual growth rate varies significantly in 2003 (see Fig. 2b) and because only N=3 data points are available for averaging in 2003. In contrast, the year 2005 growth rate uncertainty is much smaller (0.~~26~~28 ppm/year) because the growth rates vary ~~only little~~less during 2005 and because N=12 data points are available for averaging.

~~Figure 3 shows the corresponding results for the global data set. As can be seen, all time series are similar to the ones shown in Fig. 2 for northern mid-latitudes. However, there are also difference, e.g., the seasonal cycles as shown in Fig. 2a and Fig. 3a. For northern mid-latitudes (Fig. 2a) the shape of these cycles is very similar for all years in contrast to the global data shown in Fig. 3a. This is due to spatial sampling differences as the first few years (until 2008) are "land only" data as the SCIAMACHY XCO~~~~$_2$~~ ~~is limited to observations over land whereas GOSAT XCO~~~~$_2$~~ ~~(from 2009 onwards) is not restricted to land (see global maps shown in Fig. 1). For the northern mid-latitude region the land coverage dominates (see global map in Fig. 2a). Therefore, for northern mid-latitudes SCIAMACHY and GOSAT sample similar regions, in contrast to the global region (Fig. 3), where the spatial sampling differences are larger. In Fig. 3c~~In Fig. 2c also the NOAA global growth rates (Dlugokencky and Tans, 2017b) are shown. As can be seen, the satellite-derived growth rates agree well with the NOAA growth rates obtained from CO_2 surface observations. For the time period 2003-2016 the linear correlation coefficient R is 0.82 and the difference is -0.02±0.28 ppm/year (mean difference ± standard deviation). Perfect agreement is not to be expected as these two growth rate time series have been obtained from CO_2 observations, which represent very different vertical sampling of the atmosphere (surface (NOAA) versus entire vertical column (satellite)).

~~Growth rate time series for several latitude bands are shown in Fig. 4. As can be seen from Fig. 4, the growth rates are similar in all latitude bands including the global results (for numerical values see Tab. 2).~~ As can also be seen from Fig. 2c~~The reason for this is that atmospheric CO~~~~$_2$~~ ~~is long-lived and therefore well-mixed. As a result of atmospheric transport and mixing, similar mean annual CO~~~~$_2$~~ ~~growth rates, within their measurements error, are expected for all values derived at the different latitude bands. This behaviour is shown in Fig. 4 and is interpreted as an indication of the good quality of the satellite XCO~~~~$_2$~~ ~~data product and the adequacy of the method used to compute the annual mean CO~~~~$_2$~~ ~~growth rates. As can also be seen from Fig. 4~~, the largest growth rates are approximately 3 ppm/year during 2015 and 2016. These record large growth rates (Peters et al., 2017) are attributed to the consequences of the strong 2015/2016 El Niño event, which produced large CO_2 emissions from fires and enhanced net biospheric respiration in the tropics relative to normal conditions (Heymann et al., 2017; Liu et al., 2017). Many of these fires are initiated by humans, for example, to clear tropical forests. In this study, human emissions of CO_2 are defined as emissions from fossil fuel combustion and industry (Le Quéré et al., 2016, 2018) but do not include, for example, CO_2 emissions originating from slash and burn agriculture.

4 Correlation of CO_2 growth rates with fossil CO_2 emissions and ENSO indices

It is well known that changes of the growth rate of atmospheric CO_2 have anthropogenic and natural causes (e.g., Jones et al., 2001; Betts et al., 2016; Kim et al., 2016; Liu et al., 2017; Chylek et al., 2018). In this section we are aiming at answering the following question: "Assuming that the variability of the CO_2 growth rate is dominated by

ENSO and by human emissions, which of the two considered causes dominates the growth rate variability given the satellite-derived growth rates and their uncertainty?". To answer this question we are using a simple linear statistical model and time series of human emissions and two ENSO indices assuming that these indices are appropriate proxies for ENSO related effects in the context of providing a reliable answer.

Figure ~~5~~3 shows a comparison of the CO_2 annual mean growth rates (Fig. ~~5a~~3a) with annual global CO_2 emissions from fossil fuel combustion and industry (Fig. ~~5b~~3b) (Le Quéré et al., 2018; GCP 2017) (correlation of growth rate and human emissions: $R^2 = 31\%$). As can be seen, the growth rates vary significantly in recent years despite nearly constant human emissions. Figure ~~5d~~3d shows two ENSO indices: the Southern Oscillation Index (SOI, blue lines) (NOAA 2017a; Ropelewski and Jones, 1987) and the Oceanic Niño Index (ONI, green lines) (NOAA 2017b). Whereas SOI is defined as the normalized pressure difference between Tahiti and Darwin (values less than -1 indicate the presence of a strong El Niño), ONI is based on Sea Surface Temperature (SST) differences (positive values correspond to El Niño). The dotted lines correspond to the original (i.e., unshifted) annual mean indices and the solid lines correspond to time shifted ENSO indices. Time shifts have been investigated to consider the delay in atmospheric response to ENSO-induced changes. As shown in Fig. ~~5c~~3c, the growth rate response as quantified by R^2 is largest after 4 months for ONI ($R^2 = 35\%$) and after 7 months for SOI ($R^2 = 30\%$). These maxima have been adopted for the solid (shifted) lines in Fig ~~5d~~3d. This finding is consistent with results from other studies, where lags in the range 3-9 months have been reported (Jones et al., 2001; Kim et al., 2016; Chylek et al., 2018).

In order to separate and quantify the ~~impact~~contributions of the human CO_2 emissions and of ENSO, as described by the two indices SOI and ONI, ~~on~~to the growth rate variations, we employ the method of "variation partitioning" (Peres-Neto et al., 2006). ~~We~~To achieve this, we have fitted three basis functions to the 2003-2016 growth rate time series via linear least-squares minimization (we explain the method in this paragraph using SOI but the method does not depend on which ENSO index is used): (i) a constant offset (variance zero), (ii) the human CO_2 emissions (Fig. ~~5b~~3b) and (iii) SOI shifted by 7 months (blue solid line in Fig. ~~5d~~3d). The variance of the scaled emission, i.e., of the human emission scaled with the corresponding fit parameter, is 0.0758 ppm^2/year^2 (note that in this section we report numerical values with four digital places but this shall not imply that all decimal places are significant). The variance of the scaled SOI is 0.1070 ppm^2/year^2 and the variance of the fit residual is 0.0728 ppm^2/year^2. The sum of the three individual variances is 0.2557 ppm^2/year^2 whereas the variance of the annual mean growth rate is 0.2307 ppm^2/year^2. This shows that the sum of the variances is 10.8% larger than the variance of the growth rate, i.e., the sum of the variances is not exactly equal to the variance of the sum. The reason for this is that the CO_2 emission and the SOI time series are not uncorrelated ($R = 0.14$). To account for correlations, we subtract the variance of the residual from the variance of the growth rate. The result is the part of the variance to be explained by the emissions and by the SOI. The ratio of this to be explained variance (0.1579 ppm^2/year^2) and the sum of the variances of the emissions and SOI ((0.0758 + 0.1070) ppm^2/year^2 = 0.1828 ppm^2/year^2) is 0.8638. The latter is then used as a scaling factor applied to the variances of the emissions and of the SOI. The scaled variances are 0.0655 ppm^2/year^2 for the emissions and 0.0924 ppm^2/year^2 for SOI (note that the sum of these scaled variances and the variance of the residual is equal to the variance of the growth rate). From this we conclude that the human emissions explain 28% (= 0.0655/0.2307) of the variance of the growth rate and that ENSO as quantified by the SOI explains 40% (= 0.0924/0.2307). We computed (1-sigma) uncertainties of these estimates by numerically perturbing the satellite-derived annual mean growth rates taking into account their uncertainty (see

~~Fig. 4~~Figs. 2c and 3) and by subsequently repeating the computations as explained above 10,000 times. The perturbations correspond to random perturbations of the annual mean growth rates assuming normal distributions for each year and no correlation between the different years. This analysis yields that 40±13% of the growth rate variation results from the impact of ENSO and that 28±14% is due to the human emissions of CO_2. Using these simulations, we also computed the fraction of cases where the ENSO impact dominates over the human emissions. This fraction is 63% in this case, i.e., when using SOI and when the analysis is applied to the entire time period 2003-2016. This fraction is interpreted as the probability that ENSO-induced impacts on the variation of the growth rate dominates that of human emissions.

When using ONI instead of SOI, ENSO explains 37±14% of the growth rate variance during 2003-2016, human emissions explain 24±14% and the fraction where ENSO dominates is again 63%. When restricting the time period to 2010-2016, which is dominated by strong 2010/2012 La Niña events (Boening et al., 2012; Rodrigues et al., 2014) and by the strong 2015/2016 El Niño, the results are the following: Using the SOI analysis, we find that ENSO explains 58±19% of the variance, human emissions explain 2±9% and the probability that ENSO dominates is 94%. For the ONI analysis, we find that ENSO explains 59±20% of the variance, human emissions explain 3±9% and the probability that ENSO dominates is 94%. This analysis shows that the ENSO impact on CO_2 growth rate variations dominates over that of human emissions throughout the period 2003-2016 but in particular in the second half of this period, i.e., during 2010-2016.

5 Conclusions

We presented a method for the computation of atmospheric CO_2 column annual mean growth rates from satellite XCO_2 retrievals. The satellite XCO_2 data product used is the Obs4MIPs version 3 (O4Mv3) XCO_2 data product based on SCIAMACHY/ENVISAT and TANSO-FTS/GOSAT satellite data. This product covers the time period 2003-2016 and has monthly time and 5°x5° spatial resolution.

~~The presented method has been applied to the global satellite data and to selected latitude bands.~~ The estimated uncertainty of the satellite-derived annual mean growth rates is typically ~~in the range~~ 0.3~~-0.5~~ ppm/year (1-sigma~~). The global~~) with the exception of the first year 2003, where the uncertainty is 0.76 ppm/year, and of the last year 2016, where the uncertainty is 0.50 ppm/year. The growth rates agree with NOAA within the uncertainty of the satellite-derived growth rates (mean difference ± standard deviation: 0.0±0.3 ppm/year; R: 0.82). In agreement with NOAA, we find that the growth rates are largest in the years 2015 and 2016. These growth rates are around 3 ppm/year and are attributed to the 2015/2016 El Niño resulting in large CO_2 emissions from fires and enhanced net biospheric respiration in the tropics relative to normal conditions (Heymann et al., 2017; Liu et al., 2017). Our analysis also shows that the ENSO impact on CO_2 growth rate variations dominates over that of human emissions throughout the period 2003-2016 (14 years) but in particular during the period 2010-2016 (second half of the investigated time period) due to strong La Niña and El Niño events. We estimate the probability that the impact of ENSO on the variability is larger than the impact of human emissions to be 63% for the time period 2003-2016. If the time period is restricted to 2010-2016 this probability increases to 94%.

In the future, we plan to regularly update the satellite-derived XCO_2 growth rates to monitor this important quantity. This will also include satellite XCO_2 retrievals from other satellite instruments such as XCO_2 from NASA's OCO-2 mission (e.g., Eldering et al., 2017; Reuter et al., 2017c, 2017d).

References

Ballantyne, A. P., Alden, C. B., Miller, J. B., Tans, P. P., and White, J. W. C.: Increase in observed net carbon dioxide uptake by land and oceans during the last 50 years, Nature 488, 70–72, 2012.

Basu, S., Guerlet, S., Butz, A., Houweling, S., Hasekamp, O., Aben, I., Krummel, P., Steele, P., Langenfelds, R., Torn, M., Biraud, S., Stephens, B., Andrews, A., and Worthy, D.: Global CO_2 fluxes estimated from GOSAT retrievals of total column CO_2, Atmos. Chem. Phys., 13, 8695–8717, doi:10.5194/acp-13-8695-2013, 2013.

Betts, R. A., Jones, C. D., Knight, J. R., Keeling, R. F., and Kennedy, J. J., El Niño and a record CO_2 rise, Nature Climate Change, vol. 6, p. 806–810, https://www.nature.com/articles/nclimate3063.pdf , 2016.

Boening, C., Willis, J. K., Landerer, F. W., Nerem, R. S., and J. Fasullo, J.: The 2011 La Niña: So strong, the oceans fell, Geophys. Res. Lett., 38, pp. 5, doi:10.1029/2012GL053055, 2012.

Bovensmann, H., Burrows, J. P., Buchwitz, M., Frerick, J., Noël, S., Rozanov, V. V., Chance, K. V., and Goede, A. H. P.: SCIAMACHY - Mission objectives and measurement modes, J. Atmos. Sci., 56 (2), 127-150, 1999.

Buchwitz, M., de Beek, R., Noël, S., Burrows, J. P., Bovensmann, H., Schneising, O., Khlystova, I., Bruns, M., Bremer, H., Bergamaschi, P., Körner, S., and Heimann, M.: Atmospheric carbon gases retrieved from SCIAMACHY by WFM-DOAS: version 0.5 CO and CH_4 and impact of calibration improvements on CO_2 retrieval, Atmos. Chem. Phys., 6, 2727–2751, 2006.

Buchwitz, M., Schneising, O., Burrows, J. P., Bovensmann, H., Reuter, M., and Notholt, J.: First direct observation of the atmospheric CO_2 year-to-year increase from space, Atmos. Chem. Phys., 7, 4249-4256, 2007.

Buchwitz, M., Reuter, M., Schneising, O., Boesch, H., Guerlet, S., Dils, B., Aben, I., Armante, R., Bergamaschi, P., Blumenstock, T., Bovensmann, H., Brunner, D., Buchmann, B., Burrows, J. P., Butz, A., Chédin, A., Chevallier, F., Crevoisier, C. D., Deutscher, N. M., Frankenberg, C., Hase, F., Hasekamp, O. P., Heymann, J., Kaminski, T., Laeng, A., Lichtenberg, G., De Mazière, M., Noël, S., Notholt, J., Orphal, J., Popp, C., Parker, R., Scholze, M., Sussmann, R., Stiller, G. P., Warneke, T., Zehner, C., Bril, A., Crisp, D., Griffith, D. W. T., Kuze, A., O'Dell, C., Oshchepkov, S., Sherlock, V., Suto, H., Wennberg, P., Wunch, D., Yokota, T., and Yoshida, Y.: The Greenhouse Gas Climate Change Initiative (GHG-CCI): comparison and quality assessment of near-surface-sensitive satellite-derived CO_2 and CH_4 global data sets, Remote Sensing of Environment, 162, 344-362, doi:10.1016/j.rse.2013.04.024, 2015.

Buchwitz, M., Reuter, M., Schneising-Weigel, O., Aben, I., Detmers, R. G., Hasekamp, O. P., Boesch, H., Anand,, J., Crevoisier, C., and Armante, R.: Product User Guide and Specification (PUGS) – Main document, Technical Report Copernicus Climate Change Service (C3S), available from C3S website (https://climate.copernicus.eu/) and from http://www.iup.uni-bremen.de/sciamachy/NIR_NADIR_WFM_DOAS/C3S_docs/C3S_D312a_Lot6.3.1.5-v1_PUGS_MAIN_v1.3.pdf, 20/10/2017, pp. 91, 2017a.

Buchwitz, M., Reuter, M., Schneising, O., Hewson, W., Detmers, R. G., Boesch, H., Hasekamp, O. P., Aben, I., Bovensmann, H., Burrows, J. P., Butz, A., Chevallier, F., Dils, B., Frankenberg, C., Heymann, J., Lichtenberg, G., De Mazière, M., Notholt, J., Parker, R., Warneke, T., Zehner, C., Griffith, D. W. T., Deutscher, N. M., Kuze, A., Suto, H., and Wunch, D.: Global satellite observations of column-averaged carbon dioxide and methane: The GHG-CCI XCO_2 and XCH_4 CRDP3 data set, Remote Sensing of Environment, 203, 276-295, http://dx.doi.org/10.1016/j.rse.2016.12.027, 2017b.

Buchwitz, M., Reuter, M., Schneising-Weigel, O., Aben, I., Detmers, R. G., Hasekamp, O. P., Boesch, H., Anand,, J., Crevoisier, C., and Armante, R.: Product Quality Assessment Report (PQAR) – Main document, Technical Report Copernicus Climate Change Service (C3S), available from C3S website (https://climate.copernicus.eu/) and from http://www.iup.uni-bremen.de/sciamachy/NIR_NADIR_WFM_DOAS/C3S_docs/C3S_D312a_Lot6.3.1.7-v1_PQAR_MAIN_v1.1.pdf, 20/10/2017, pp. 103, 2017c.

Buchwitz, M., Dils, B., Boesch, H., Brunner, D., Butz, A., Crevoisier, C., Detmers, R., Frankenberg, C., Hasekamp, O., Hewson, W., Laeng, A., Noël, S., Notholt, J., Parker, R., Reuter, M., Schneising, O., Somkuti, P., Sundström, A.-M., De Wachter, E.: ESA Climate Change Initiative (CCI) Product Validation and Intercomparison Report (PVIR) for the Essential Climate Variable (ECV) Greenhouse Gases (GHG) for data set Climate Research Data Package No. 4 (CRDP#4), Technical Report, version 5, 9-Feb-2017, link: http://www.esa-ghg-cci.org/?q=webfm_send/352, pp. 253, 2017d.

Burrows, J. P., Hölzle, E., Goede, A. P. H., Visser, H., and Fricke, W.: SCIAMACHY—Scanning Imaging Absorption Spectrometer for Atmospheric Chartography, Acta Astronaut., 35(7), 445–451, doi:10.1016/0094-5765(94)00278-t, 1995.

Butz, A., Guerlet, S., Hasekamp, O., Schepers, D., Galli, A., Aben, I., Frankenberg, C., Hartmann, J.-M., Tran, H., Kuze, A., Keppel-Aleks, G., Toon, G., Wunch, D., Wennberg, P., Deutscher, N., Griffith, D., Macatangay, R., Messerschmidt, J., Notholt, J., and Warneke, T.: Toward accurate CO_2 and CH_4 observations from GOSAT, Geophys. Res. Lett., doi:10.1029/2011GL047888, 2011.

Chevallier, F., Palmer, P. I., Feng, L., Boesch, H., O'Dell, C. W., and Bousquet, P.: Towards robust and consistent regional CO_2 flux estimates from in situ and space-borne measurements of atmospheric CO_2, Geophys. Res. Lett., 41, 1065–1070, doi:10.1002/2013GL058772, 2014.

Chylek, P., Tans, P., Christy, P., and Dubey, M. K.: The carbon cycle response to two El Nino types: an observational study, Environ. Res. Lett., 13, pp. 8, https://doi.org/10.1088/1748-9326/aa9c5b, 2018.

Cogan, A. J., Boesch, H., Parker, R. J., Feng, L., Palmer, P. I., Blavier, J.-F. L., Deutscher, N. M., Macatangay, R., Notholt, J., Roehl, C., Warneke, T., and Wunsch, D.: Atmospheric carbon dioxide retrieved from the Greenhouse gases Observing SATellite (GOSAT): Comparison with ground-based TCCON observations and GEOS-Chem model calculations, J. Geophys. Res., 117, D21301, doi:10.1029/2012JD018087, 2012.

Dlugokencky, E., and Tans, P.: Trends in atmospheric carbon dioxide. National Oceanic & Atmospheric Administration, Earth System Research Laboratory (NOAA/ESRL), 2017a.

Dlugokencky, E., and Tans, P.: Trends in atmospheric carbon dioxide, National Oceanic & Atmospheric Administration, Earth System Research Laboratory (NOAA/ESRL), file: ftp://aftp.cmdl.noaa.gov/products/trends/co2/co2_gr_gl.txt (access: 24 November 2017), 2017b.

Eldering, A. et al. The Orbiting Carbon Observatory-2: first 18 months of science data products, Atmos. Meas. Tech., 10, 549-563, https://doi.org/10.5194/amt-10-549-2017, 2017.

GCP: Global CO_2 emissions from Global Carbon Project (GCP) website (http://www.globalcarbonproject.org/carbonbudget/17/data.htm), main data source: Thomas Boden, Gregg Marland, Robert Andres 2017 (CDIAC), GCP-CICERO, UNFCCC, BP Statistical Review of World Energy (BP, 2017), US Geological Survey (USGS, 2017), 2017.

Hakkarainen, J., Ialongo, I., and Tamminen, J.: Direct space-based observations of anthropogenic CO_2 emission areas from OCO-2, Geophys. Res. Lett., 43, 11,400–11,406, doi:10.1002/2016GL070885, 2016.

Heymann, J., Reuter, M., Buchwitz, M., Schneising, O., Bovensmann, H., Burrows, J. P., Massart, S., Kaiser, J. W., and Crisp, D.: CO_2 emission of Indonesian fires in 2015 estimated from satellite-derived atmospheric CO_2 concentrations, Geophys. Res. Lett., doi:10.1002/2016GL072042, pp. 18, 2017.

Houweling, S., Baker, D., Basu, S., Boesch, H., Butz, A., Chevallier, F., Deng, F., Dlugokencky, E. J., Feng, L., Ganshin, A., Hasekamp, O., Jones, D., Maksyutov, S., Marshall, J., Oda, T., O'Dell, C. W., Oshchepkov, S., Palmer, P. I., Peylin, P., Poussi, Z., Reum, F., Takagi, H., Yoshida, Y., and Zhuralev, R.: An intercomparison of inverse models for estimating sources and sinks of CO_2 using GOSAT measurements, J. Geophys. Res. Atmos., 120, 5253–5266, doi:10.1002/2014JD022962, 2015.

Huntzinger, D. N., Michalak, A. M., Schwalm, C., Ciais, P., King, A. W., Fang, Y., Schaefer, K., Wei, Y., Cook, R. B., Fisher, J. B., Hayes, D., Huang, M., Ito, A., Jain, A. K., Lei, H., Lu, C., Maignan, F., Mao, J., Parazoo, N., Peng, S., Poulter, B., Ricciuto, D., Shi, X., Tian, H., Wang, W., Zeng, N., and Zhao, F.: Uncertainty in the response of terrestrial carbon sink to environmental drivers undermines carbon-climate feedback predictions, Nature, Scientific Reports, 7: 4765, doi:10.1038/s41598-017-03818-2, 2017.

IPCC: Climate Change 2013: The Physical Science Basis, Working Group I Contribution to the Fifth Assessment Report of the Intergovernmental Report on Climate Change, http://www.ipcc.ch/report/ar5/wg1/, Cambridge University Press, 2013.

Jones, C. D., Collins, M., Cox, P. M., and Spall, S. A.: The Carbon Cycle Response to ENSO: A Coupled Climate-Carbon Cycle Model Study, Journal of Climate, Vol. 14, 4113-4129, 2001.

Kaminski, T., Scholze, M., Voßbeck, M., Knorr, W., Buchwitz, M, and Reuter, M.: Constraining a terrestrial biosphere model with remotely sensed atmospheric carbon dioxide, Remote Sensing of Environment 203, 109-124, 2017.

Kim, J.-S., Kug, J.-S., Yoon, J.-H., Jeong, S.-J., Increased Atmospheric CO_2 Growth Rate during El Niño Driven by Reduced Terrestrial Productivity in the CMIP5 ESMs, Journal of Climate, 8783-8805, 29. 10.1175/JCLI-D-14-00672.1, 2016.

Kort, E., Frankenberg, C., Miller, C. E., and Oda, T.: Space-based observations of megacity carbon dioxide. Geophys. Res. Lett., 39, doi:10.1029/2012GL052738, 2012.

Kuze, A., Suto, H., Shiomi, K., Kawakami, S., Tanaka, M., Ueda, Y., Deguchi, A., Yoshida, J., Yamamoto, Y., Kataoka, F., Taylor, T. E., and Buijs, H. L.: Update on GOSAT TANSO-FTS performance, operations, and data products after more than 6 years in space, Atmos. Meas. Tech., 9, 2445-2461, doi:10.5194/amt-9-2445-2016, 2016.

Lauer, A., Eyring, V., Righi, M., Buchwitz, M., Defourny, P., Evaldsson, M., Friedlingstein, P., de Jeu, R., de Leeuw, G., Loew, A., Merchant, C. J., Müller, B., Popp, T., Reuter, M., Sandven, S., Senftleben, D., Stengel, M., Van Roozendael, M., Wenzel, S., and Willén, U.: Benchmarking CMIP5 models with a subset of ESA CCI Phase 2 data using the ESMValTool, Remote Sensing of Environment, 203, 9-39, http://dx.doi.org/10.1016/j.rse.2017.01.007, 2017.

Le Quéré, C., Andrew, R. M., Canadell, J. G., Sitch, S., Korsbakken, J. I., Peters, G. P., Manning, A. C., Boden, T. A., Tans, P. P., Houghton, R. A., Keeling, R. F., Alin, S., Andrews, O. D., Anthoni, P., Barbero, L., Bopp, L., Chevallier, F., Chini, L. P., Ciais, P., Currie, K., Delire, C., Doney, S. C., Friedlingstein, P., Gkritzalis, T., Harris, I., Hauck, J., Haverd, V., Hoppema, M., Klein Goldewijk, K., Jain, A. K., Kato, E., Körtzinger, A., Landschützer, P., Lefèvre, N., Lenton, A., Lienert, S., Lombardozzi, D., Melton, J. R., Metzl, N., Millero, F., Monteiro, P. M. S., Munro, D. R., Nabel, J. E. M. S., Nakaoka, S. I., O'Brien, K., Olsen, A., Omar, A. M., Ono, T., Pierrot, D., Poulter, B., Rödenbeck, C., Salisbury, J., Schuster, U., Schwinger, J., Séférian, R., Skjelvan, I., Stocker, B. D., Sutton, A. J., Takahashi, T., Tian, H., Tilbrook, B., van der Laan-Luijkx, I. T., van der Werf, G. R., Viovy, N., Walker, A. P., Wiltshire, A. J., and Zaehle, S.: Global Carbon Budget 2016, Earth Syst. Sci. Data, 8, 605-649, 2016.

Le Quéré, C., Andrew, R. M., Friedlingstein, P., Sitch, S., Pongratz, J., Manning, A. C., Korsbakken, J. I., Peters, G. P. Canadell, J. G., Jackson, R. B., Boden, T. A., Tans, P. P., Andrews, O. D., Arora, V. K., Bakker, D. D. E, Barbero, L., Becker, M., Betts, R. A., Bopp, L., Chevallier, F., Chini, L. P., Ciais, P., Cosca, C. E., Cross, J., Currie, K., Gasser, T., Harris, I., Hauck, J., Haverd, V., Houghton, R. A., Hunt, C. W., Hurtt, G., Ilyina, T., Jain, A. K., Kato, E., Kautz, M., Keeling, R. F., Goldewijk, K. K., Körtzinger, A., Landschützer, P., Lefèvre, N., Lenton, A., Lienert, S., Lima, I., Lombardozzi, D., Metzl, N., Millero, F., Monteiro, P. M. S., Munro, D. R., Nabel, J. E. M. S., Nakaoka, S., Nojiri, Y., Padín, X. A., Peregon, A., Pfeil, B., Pierrot, D., Poulter, B., Rehder, G., Reimer, J., Rödenbeck, C., Schwinger, J., Séférian, R., Skjelvan, I., Stocker, B. D., Tian, H., Tilbrook, B., van der Laan-Luijkx, I. T., van der Werf, G. R., van Heuven, S., Viovy, N., Vuichard, N., Walker, A. P., Watson, A. J., Wiltshire, A. J., Zaehle, S., and Zhu, D.: Global Carbon Budget 2017, Earth System Science Data, 10, 405-448, DOI: 10.5194/essd-10-405-2018, 2018.

Liu, J., Bowman, K. W., Schimel, D. S., Parazoo, N. C., Jiang, Z., Lee, M., Bloom, A. A., Wunch, D., Frankenberg, C., Sun, Y., O'Dell, C. W., Gurney, K. R., Menemenlis, D., Gierach, M., Crisp, D., and Eldering, A.: Contrasting carbon cycle responses of the tropical continents to the 2015–2016 El Niño, Science, 358, eaam5690, pp. 7, 2017.

Maksyutov, S., Takagi, H., Valsala, V. K., Saito, M., Oda, T., Saeki, T., Belikov, D. A., Saito, R., Ito, A., Yoshida, Y., Morino, I., Uchino, O., Andres, R. J., and Yokota, T.: Regional CO_2 flux estimates for 2009–2010 based on GOSAT and ground-based CO_2 observations, Atmos. Chem. Phys., 13, 9351-9373, 2013.

Nassar, R., Hill, T. G., McLinden, C. A., Wunch, D., Jones, D. B. A., and Crisp, D.: Quantifying CO_2 emissions from individual power plants from space, Geophys. Res. Lett., doi:10.1002/2017GL074702, 2017.

NIES: Recent global CO_2 (http://www.gosat.nies.go.jp/en/recent-global-co2.html), 2017.

NOAA: Southern Oscillation Index (SOI), file https://www.esrl.noaa.gov/psd/gcos_wgsp/Timeseries/Data/soi.long.data, data based on the method of Ropelewski and Jones, 1987, using data from the Climate Research Unit (CRU; http://www.cru.uea.ac.uk/cru/data/soi/), 2017a.

NOAA: Oceanic Niño Index (ONI), file https://www.esrl.noaa.gov/psd/data/correlation/oni.data obtained from https://www.esrl.noaa.gov/psd/data/climateindices/list, 2017b.

O'Dell, C. W., Connor, B., Bösch, H., O'Brien, D., Frankenberg, C., Castano, R., Christi, M., Eldering, D., Fisher, B., Gunson, M., McDuffie, J., Miller, C. E., Natraj, V., Oyafuso, F., Polonsky, I., Smyth, M., Taylor, T., Toon, G. C.,Wennberg, P. O., andWunch, D.: The ACOS CO_2 retrieval algorithm – Part 1: The ACOS CO_2 retrieval algorithm – Part 1: Description and validation against synthetic observations, Atmos. Meas. Tech., 5, 99–121, doi:10.5194/amt-5-99-2012, 2012.

Parker, R. J., Boesch, H., Wooster, M. J., Moore, D. P., Webb, A. J., Gaveau, D., and Murdiyarso, D.: Atmospheric CH_4 and CO_2 enhancements and biomass burning emission ratios derived from satellite observations of the 2015 Indonesian fire plumes, Atmos. Chem. Phys., 16, 10111-10131, doi:10.5194/acp-16-10111-2016, 2016.

Peres-Neto, P. R., Legendre, P., Dray, S., and Borcard, D.: Variation partitioning of species data matrices: Estimation and comparison of fractions, Ecology, 87(19), pp. 2614-2625, 2006.

Peters, W., Jacobson, A. R., Sweeney, C., Andrews, A. E., Conway, T. J., Masarie, K., Miller, J. B., Bruhwiler, L. M. P., Pétron, G., Hirsch, A. I., Worthy, D. E. J., van der Werf, G. R., Randerson, J. T., Wennberg, P. O., Krol, M. C., and Tans, P. P.: An atmospheric perspective on North American carbon dioxide exchange: CarbonTracker, Proc. Natl. Acad. Sci. USA, 104, 18925–18930, doi:10.1073/pnas.0708986104, 2007.

Peters, G. P., Le Quéré, C., Andrew, R. M., Canadell, J. G., Friedlingstein, P., Ilyina, T., Jackson, R., Joos, F., Korsbakken, J. I., McKinley, G. A., Sitch, S., and Tans, P.: Towards real-time verification of CO_2 emissions, Nature Climate Change, 13 November 2017, doi:10.1038/s41558-017-0013-9, 2017.

Peylin, P., Law, R. M., Gurney, K. R., Chevallier, F., Jacobson, A. R., Maki, T., Niwa, Y., Patra, P. K., Peters, W., Rayner, P. J., Rödenbeck, C., van der Laan-Luijkx, I. T., and Zhang, X.: Global atmospheric carbon budget: results from an ensemble of atmospheric CO_2 inversions, Biogeosciences, 10, 6699–6720, doi:10.5194/bg-10-6699-2013, 2013.

Reuter, M., Bovensmann, H., Buchwitz, M., Burrows, J. P., Connor, B. J., Deutscher, N. M., Griffith, D. W. T., Heymann, J., Keppel-Aleks, G., Messerschmidt, J., Notholt, J., Petri, C., Robinson, J., Schneising, O., Sherlock, V., Velazco, V., Warneke, W., Wennberg, P. O., and Wunch, D.: Retrieval of atmospheric CO_2 with enhanced accuracy and precision from SCIAMACHY: Validation with FTS measurements and comparison with model results, J. Geophys. Res., 116, D04301, doi:10.1029/2010JD015047, 2011.

Reuter, M., H. Boesch, H. Bovensmann, A. Bril, M. Buchwitz, A. Butz, J. P. Burrows, C. W. O'Dell, S. Guerlet, O. Hasekamp, J. Heymann, N. Kikuchi, S. Oshchepkov, R. Parker, S. Pfeifer, O. Schneising, T. Yokota, and Y.

Yoshida: A joint effort to deliver satellite retrieved atmospheric CO_2 concentrations for surface flux inversions: the ensemble median algorithm EMMA, Atmos. Chem. Phys., 13, 1771-1780, 2013.

Reuter, M., Buchwitz, M., Hilker, M., Heymann, J., Schneising, O., Pillai, D., Bovensmann, H., Burrows, J. P., Bösch, H., Parker, R., Butz, A., Hasekamp, O., O'Dell, C. W., Yoshida, Y., Gerbig, C., Nehrkorn, T., Deutscher, N. M., Warneke, T., Notholt, J., Hase, F., Kivi, R., Sussmann, R., Machida, T., Matsueda, H., and Sawa, Y.: Satellite-inferred European carbon sink larger than expected, Atmos. Chem. Phys., 14, 13739-13753, 2014a.

Reuter, M., Buchwitz, M., Hilboll, A., Richter, A., Schneising, O., Hilker, M., Heymann, J., Bovensmann, H., and Burrows, J. P.: Decreasing emissions of NOx relative to CO_2 in East Asia inferred from satellite observations, Nature Geoscience, 28 Sept. 2014, doi:10.1038/ngeo2257, pp. 4, 2014b.

Reuter, M., Buchwitz, M., Schneising, O., Noël, S., Rozanov, V., Bovensmann, H., and Burrows, J. P.: A Fast Atmospheric Trace Gas Retrieval for Hyperspectral Instruments Approximating Multiple Scattering - Part 1: Radiative Transfer and a Potential OCO-2 XCO_2 Retrieval Setup, Remote Sens., 9, 1159, doi:10.3390/rs9111159, 2017c.

Reuter, M., Buchwitz, M., Schneising, O., Noël, S., Bovensmann, H., and Burrows, J. P.: A Fast Atmospheric Trace Gas Retrieval for Hyperspectral Instruments Approximating Multiple Scattering - Part 2: Application to XCO_2 Retrievals from OCO-2, Remote Sens., 9, 1102, doi:10.3390/rs9111102, 2017d.

Reuter, M., Buchwitz, M., and Schneising-Weigel, O.: Algorithm Theoretical Basis Document (ATBD) – ANNEX D for products XCO2_EMMA and XCH4_EMMA. Technical Report Copernicus Climate Change Service (C3S), available from C3S website (https://climate.copernicus.eu/) and from http://www.iup.uni-bremen.de/sciamachy/NIR_NADIR_WFM_DOAS/C3S_docs/C3S_D312a_Lot6.2.1.2-v1_ATBD_ANNEX-D_v1.1.pdf, 20/10/2017, pp. 32, 2017e.

Rodrigues, R. R., and McPhaden, M. J.: Why did the 2011-2012 La Niña cause a severe drought in the Brazilian Northeast? Geophys. Res. Lett., 41, 1012–1018, doi:10.1002/2013GL058703, 2014.

Ropelewski, C. F., and Jones, P. D.: An extension of the Tahiti-Darwin Southern Oscillation Index. Monthly Weather Review, 115, 2161-2165, 1987.

Schneising, O., Heymann, J., Buchwitz, M., Reuter, M., Bovensmann, H., and Burrows, J. P.: Anthropogenic carbon dioxide source areas observed from space: assessment of regional enhancements and trends, Atmos. Chem. Phys., 13, 2445-2454, doi:10.5194/acp-13-2445-2013, 2013.

Schneising, O., Reuter, M., Buchwitz, M., Heymann, J., Bovensmann, H., and Burrows, J. P.: Terrestrial carbon sink observed from space: variation of growth rates and seasonal cycle amplitudes in response to interannual surface temperature variability, Atmos. Chem. Phys., 14, 133-141, 2014.

Thoning, K. W., Tans, P. P., and Komhyr, W. D.: Atmospheric carbon dioxide at Mauna Loa Observatory, 2. Analysis of the NOAA/GMCC data. 1974-1985, J. Geophys. Res., 94, 8549-8565, 1989.

Wieder, W. R., Cleveland, C. C., Smith, W. K., and Todd-Brown, K.: Future productivity and carbon storage limited by terrestrial nutrient availability, Nature Geoscience, doi:10.1038/NGEO2313, 2015.

Wunch, D., Toon, G. C., Blavier, J.-F. L., Washenfelder, R. A., Notholt, J., Connor, B. J., Griffith, D. W. T., Sherlock, V., and Wennberg, P. O.: The Total Carbon Column Observing Network. Phil. Trans. R. Soc. A, 369, 2087–2112, doi:10.1098/rsta.2010.0240, 2011.

Wunch, D., Toon, G. C., Sherlock, V., Deutscher, N. M, Liu, X., Feist, D. G., and Wennberg, P. O.: The Total Carbon Column Observing Network's GGG2014 Data Version, Carbon Dioxide Information Analysis Center, Oak Ridge National Laboratory, Oak Ridge, Tennessee, USA, available at: doi:10.14291/tccon.ggg2014.documentation.R0/1221662, 2015.

Yoshida, Y., Kikuchi, N., Morino, I., Uchino, O., Oshchepkov, S., Bril, A., Saeki, T., Schutgens, N., Toon, G. C., Wunch, D., Roehl, C. M., Wennberg, P. O., Griffith, D. W. T, Deutscher, N. M., Warneke, T., Notholt, J., Robinson, J., Sherlock, V., Connor, B., Rettinger, M., Sussmann, R., Ahonen, P., Heikkinen, P., Kyrö, E., Mendonca, J., Strong, K., Hase, F., Dohe, S., and Yokota, T.: Improvement of the retrieval algorithm for GOSAT SWIR XCO_2 and XCH_4 and their validation using TCCON data, Atmos. Meas. Tech., 6, 1533–1547, doi:10.5194/amt-6-1533-2013, 2013.

Acknowledgements

This study has been funded in parts by the European Space Agency (ESA) (via the GHG-CCI project of ESA's Climate Change Initiative (CCI, http://www.esa-ghg-cci.org/)), by the European Union (EU) (via the Copernicus Climate Change Service (C3S, https://climate.copernicus.eu/) managed by the European Centre for Medium-range Weather Forecasts (ECMWF)) and by the State and the University of Bremen. The University of Leicester GOSAT retrievals used the ALICE High Performance Computing Facility at the University of Leicester. We thank ESA/DLR for providing us with SCIAMACHY Level 1 data products and JAXA for GOSAT Level 1B data. We also thank ESA for making these GOSAT products available via the ESA Third Party Mission archive. We thank NIES for the operational GOSAT XCO_2 Level 2 product and the NASA/ACOS team for the GOSAT ACOS Level 2 XCO_2 product. We also thank NOAA for the global CO_2 growth rates (file: ftp://aftp.cmdl.noaa.gov/products/trends/co2/co2_gr_gl.txt; access: 24-Nov-2017~~).~~) and for the Mauna Loa (MLO) CO_2 growth rates (file: ftp://aftp.cmdl.noaa.gov/products/trends/co2/co2_gr_mlo.txt; access: 9-Aug-2018). The fossil fuel and industry CO_2 emissions have been obtained from the Global Carbon Project website (http://www.globalcarbonproject.org/carbonbudget/17/data.htm; access: 20-Nov-2017). The Southern Oscillation Index (SOI) data have been obtained from NOAA (file https://www.esrl.noaa.gov/psd/gcos_wgsp/Timeseries/Data/soi.long.data; access: 20-Nov-2017). The Oceanic Niño Index (ONI) data have also been obtained from NOAA (file https://www.esrl.noaa.gov/psd/data/correlation/oni.data). And last but not least, we thank two anonymous referees for helpful comments.

Author contributions

M.B. supported by O.S., M.R., H.Bov., S.N., B.G., J.P.B.: design, data analysis, interpretation and writing of the paper. The paper has been significantly improved by: H.Boe., J.A., R.J.P., P.S., R.G.D., O.P.H., I.A., A.B., A.K., H.S., Y.Y., D.C., C.O'D. Satellite input data have been provided by: M.R., M.B., O.S. (SCIAMACHY products) and H.Boe., J.A., R.J.P., P.S., R.G.D., O.P.H., I.A., A.B., A.K., H.S., Y.Y., D. C., C.O'D. (GOSAT products).

Data availability. The O4Mv3 XCO_2 data product (but also the underlying EMMAv3 product and those individual sensor Level 2 input products which have been generated with European retrieval algorithms) ~~will be~~are available ~~(around June 2018)~~ via the Copernicus Climate Change Service (C3S, https://climate.copernicus.eu/) Climate Data Store (CDS~~).~~, https://cds.climate.copernicus.eu/). Earlier versions are available from the GHG-CCI website (http://www.esa-ghg-cci.org/) of the European Space Agency (ESA) Climate Change Initiative (CCI, e.g., Obs4MIPs version 2 (O4Mv2) covering the years 2003-2015).

Competing financial interests

The authors declare no competing financial interests.

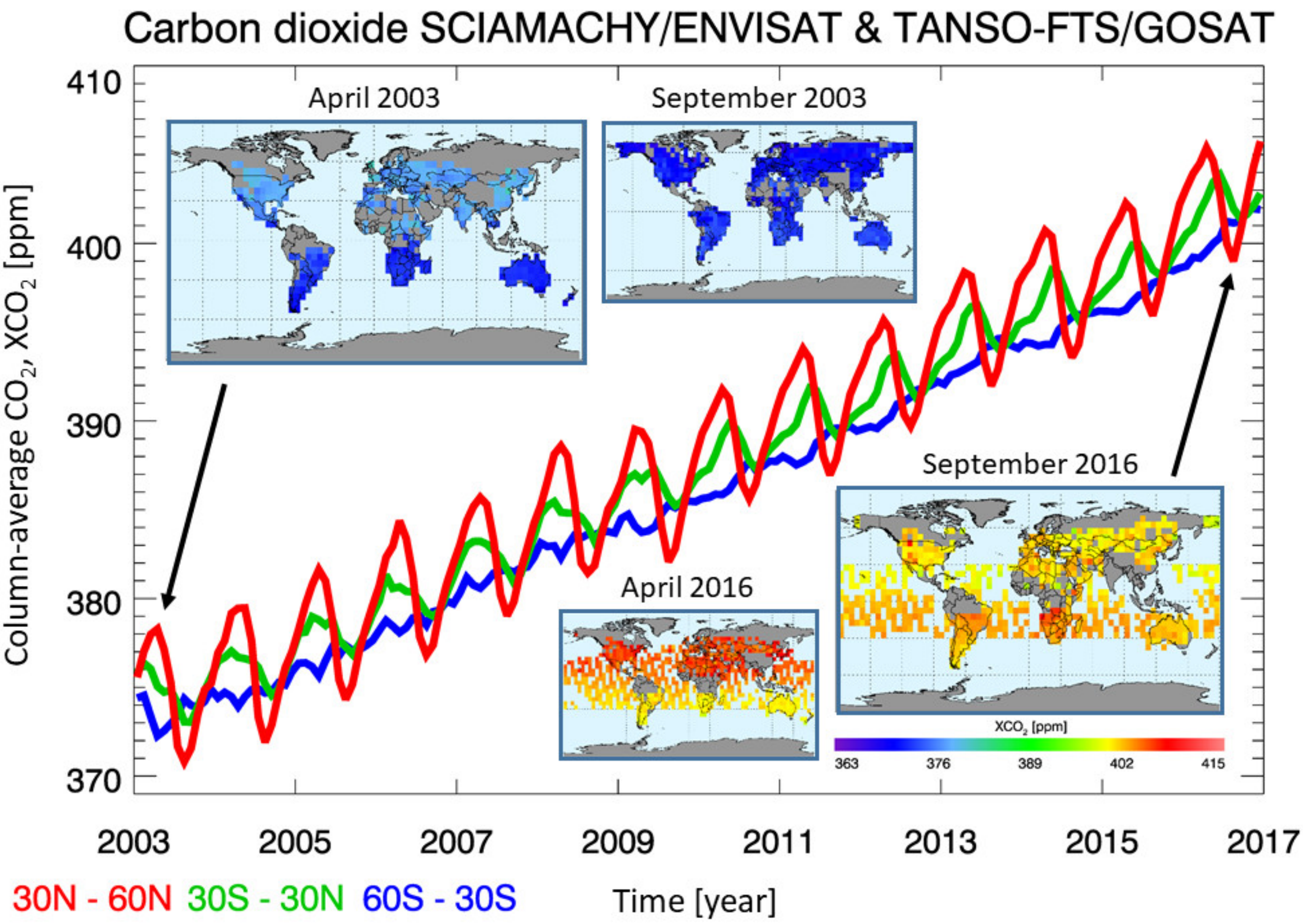

Figure 1. Time series and global maps of satellite-derived column-average dry-air mole fractions of carbon dioxide, i.e., XCO_2. Shown is data product Obs4MIPs version 3 (O4Mv3) based on an ensemble of SCIAMACHY/ENVISAT (until April 2012) and TANSO-FTS/GOSAT (since mid 2009) individual sensor / individual soundings (Level 2) data products. The three time series correspond to three latitude bands: 30°N-60°N (red), 30°S-30°N (green) and 60°S-30°S (blue). The maps in the top left show monthly XCO_2 for April and September 2003 (SCIAMACHY, land only) and the maps on the bottom right show monthly XCO_2 for April and September 2016 (TANSO-FTS, land and ocean glint).

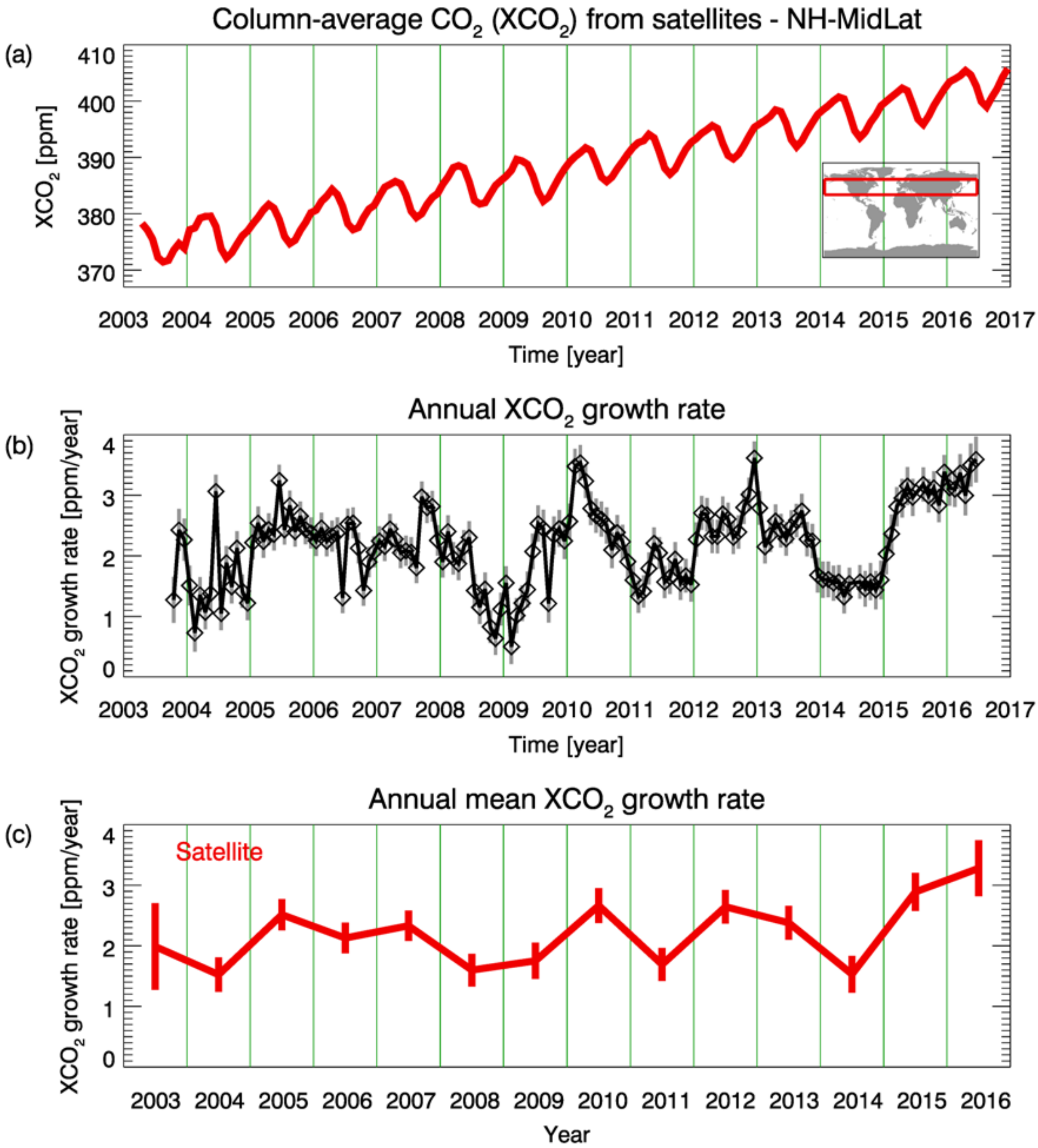

Previous Fig. 2 removed.

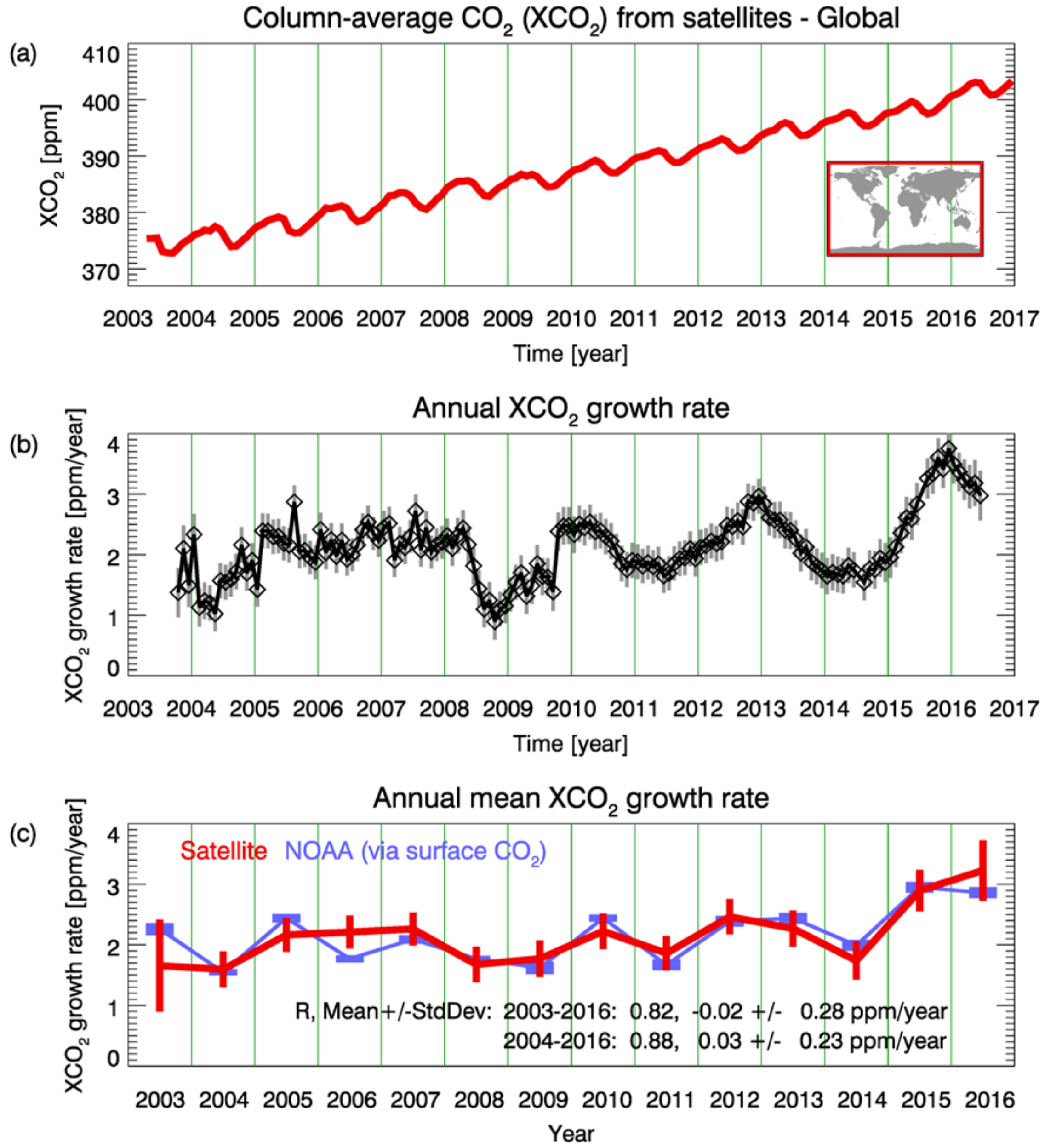

Figure 2. Atmospheric CO_2 and corresponding growth rates~~ for northern mid-latitudes.~~. (a) Monthly mean XCO_2 (red line) ~~for northern mid-latitudes~~as obtained from averaging XCO_2 data product O4Mv3 ~~in the latitude band 30°N-60°N (see red rectangle in global map).~~globally for each month. (b) Monthly sampled annual CO_2 growth rates as computed from the red curve shown in (a) including 1-sigma uncertainty (grey vertical bars). (c) Annual mean growth rates computed from averaging the values shown in (b) including 1-sigma error estimates (vertical bars) (the numerical values are listed in Tab. ~~2).~~ A1 of Annex A). The NOAA annual mean global growth rate is also shown in (c) for comparison (in blue). Also listed in (c) is the linear correlation coefficient (R), the mean difference and the standard deviation of the difference of the satellite and the NOAA growth rates for 2003-2016 and for 2004-2016.

Was previous Fig. 3. Caption is from previous Fig.2.

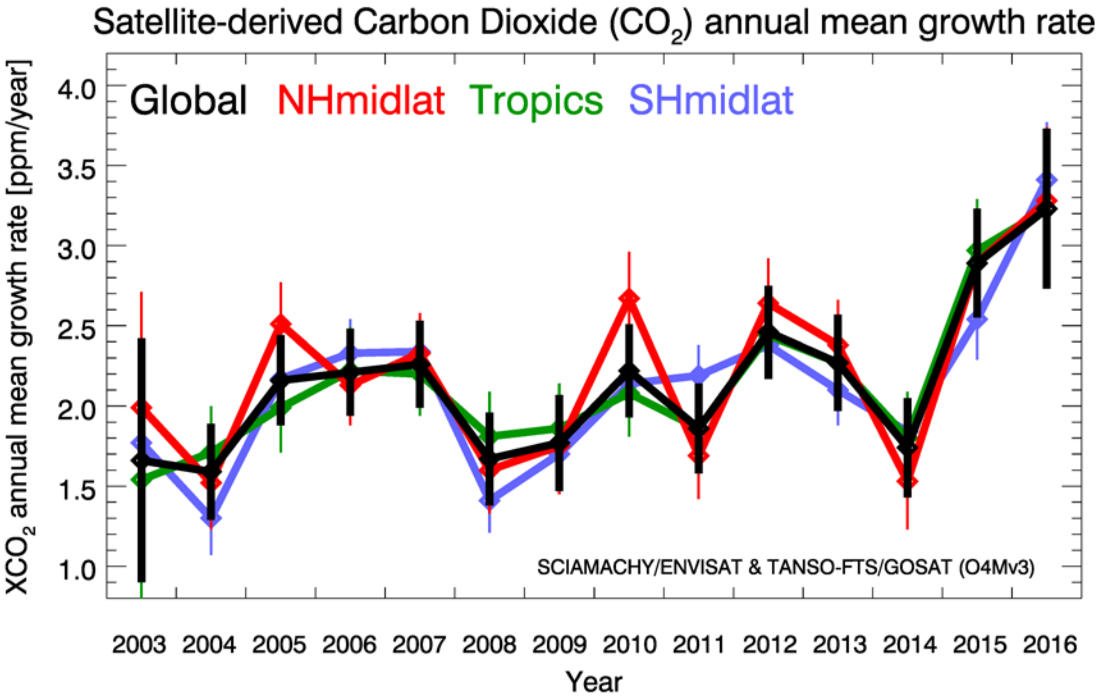

~~**Figure 4.**~~
Moved to Annex A

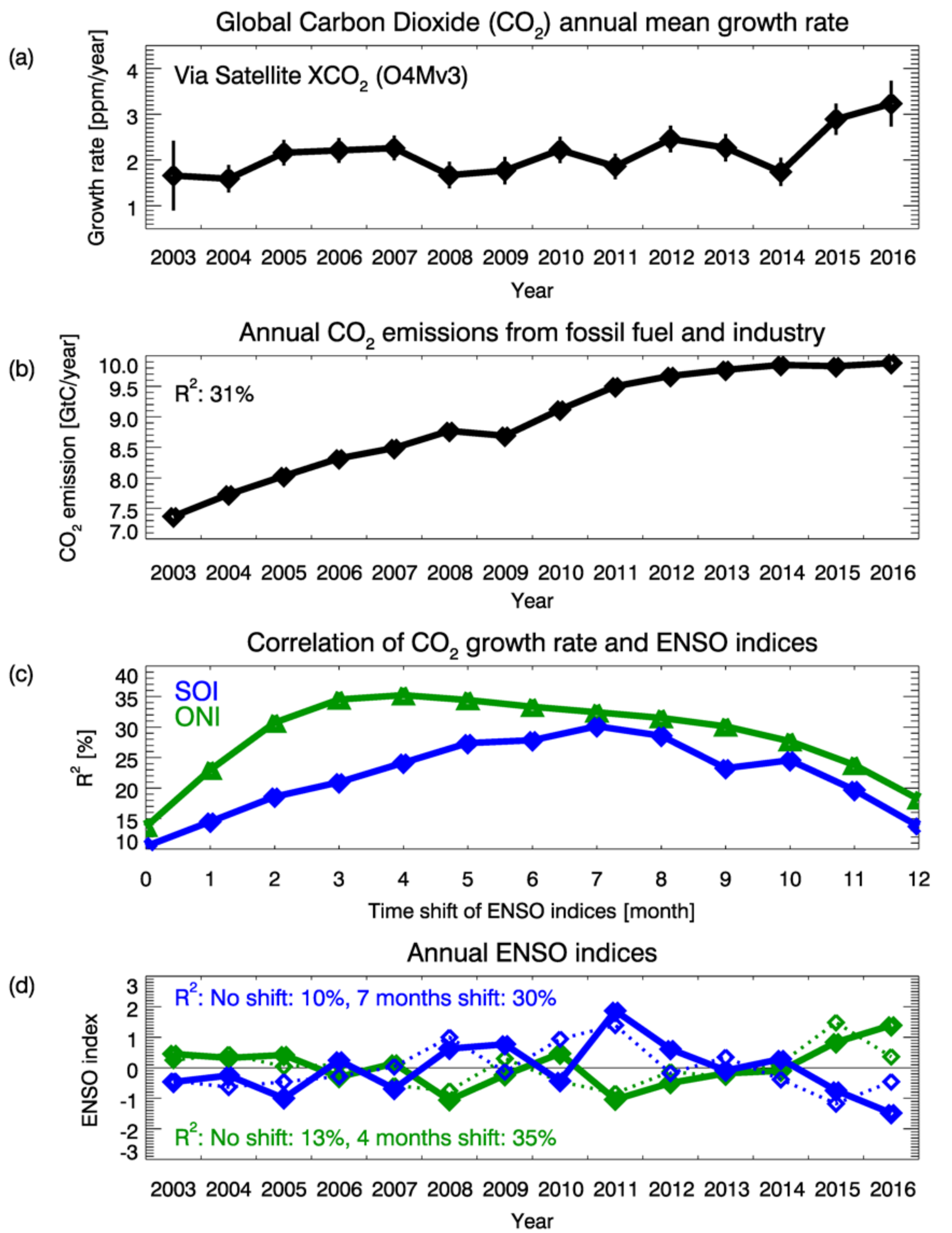

Figure 3. Carbon dioxide global annual mean growth rates compared with human emissions and ENSO indices. (a) Satellite-derived global annual mean growth rates (~~same as black line in Fig. 4).~~with 1-sigma uncertainty range shown as vertical lines). (b) CO_2 emissions from fossil fuel and industry (the correlation with the growth rate is R^2 = 31%). (c) Correlation in terms of R^2 of growth rate and annual SOI (blue curve) and ONI (green curve) as a function of time shift in months. (d) Annual SOI for no shift (blue dotted line, R^2 = 10%) and for a shift of 7 months (blue solid line, R^2 = 30%) and annual ONI for no shift (green dotted line, R^2 = 13%) and for a shift of 4 months (green solid line, R^2 = 35%).

Was previous Fig. 5. Error bars added to (a).

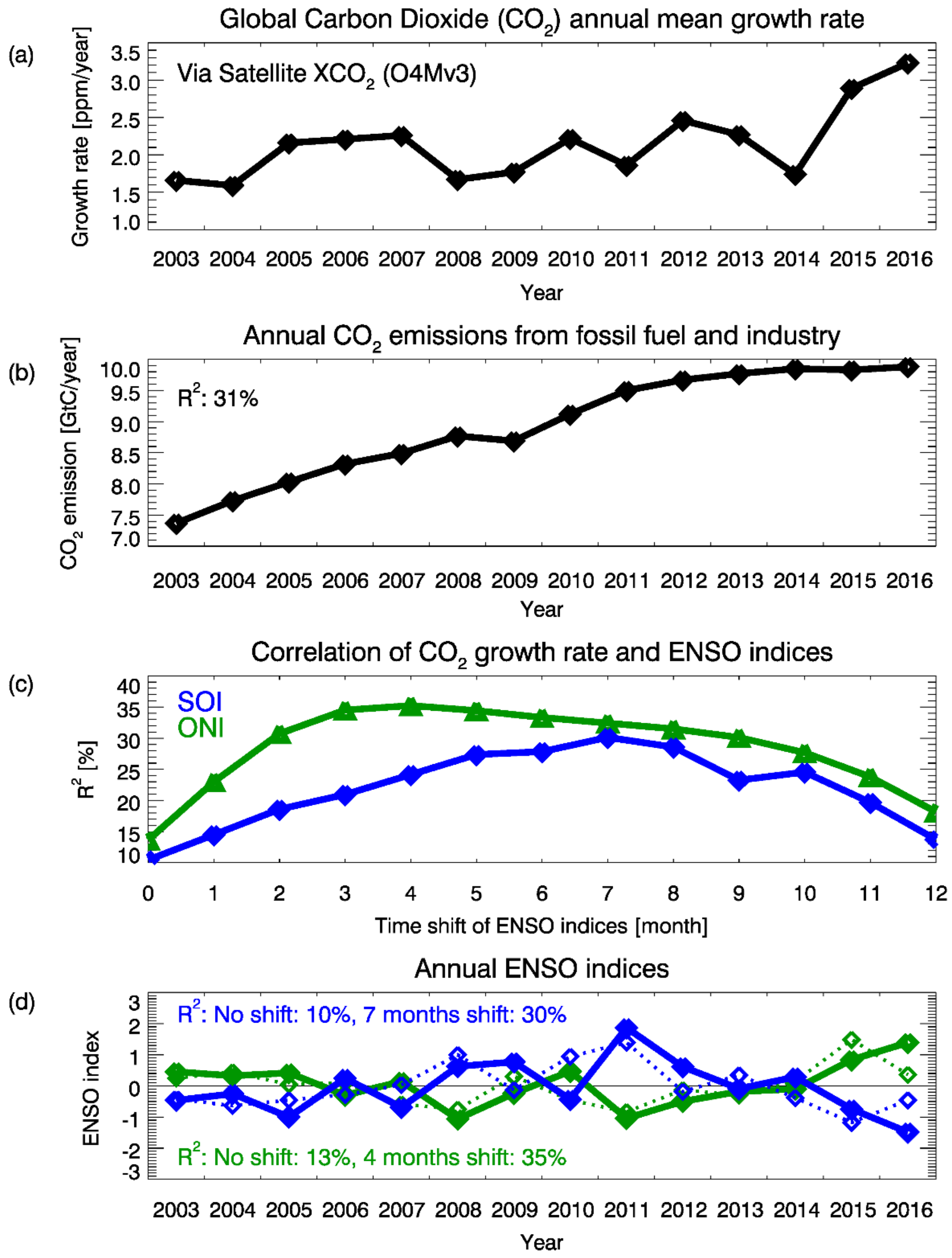

~~**Figure 5.**~~

Previous Fig. 5 (removed).

Table 1. Satellite XCO_2 data products. Individual satellite sensor XCO_2 algorithms and corresponding Level 2 data products used for generating the EMMAv3 Level 2 (i.e., individual soundings) data product, which has been gridded to obtain the O4Mv3 Level 3 data product used in this study. GHG-CCI refers to the GHG-CCI project of ESA's Climate Change Initiative (http://www.esa-ghg-cci.org/) and C3S is the Copernicus Climate Change Service (https://climate.copernicus.eu/).

Algorithm (Version)	**Sensor**	**Comment**	**Reference**
BESD (v02.01.02)	SCIAMACHY / ENVISAT	GHG-CCI / C3S product ID: CO2_SCI_BESD	Reuter et al., 2011
RemoTeC (v2.3.8)	TANSO-FTS / GOSAT	GHG-CCI / C3S product ID: CO2_GOS_SRFP	Butz et al., 2011
UoL-FP (v7.1)	TANSO-FTS / GOSAT	GHG-CCI / C3S product ID: CO2_GOS_OCFP	Cogan et al., 2012
ACOS (v7.3.10a)	TANSO-FTS / GOSAT	NASA's GOSAT XCO_2 product	O'Dell et al., 2012
NIES (v02)	TANSO-FTS / GOSAT	Operational GOSAT product	Yoshida et al., 2013

Previous Tab. 2 moved to Annex A.

Annex A

Growth rate time series have also been computed for several latitude bands as shown in Fig. A1. As can be seen, the growth rates agree within their 1-sigma uncertainty range in all latitude bands including the global results (for numerical values see Tab. A1).

The reason for this is that atmospheric CO_2 is long-lived and therefore well-mixed. Because of this we expect similar annual mean CO_2 growth rates, i.e., agreement within measurement error, for the different latitude bands and globally. Identical growth rates are not expected due to differences in the sources and sinks and the time needed for transport and mixing. The expectation of similar growth rates is corroborated by Fig. A2, which shows a comparison of the uncertainty of the satellite-derived growth rates (red bars) with the difference of two annual mean CO_2 growth rate time series from NOAA, namely the time series from Mauna Loa, Hawaii, and the global time series obtained from globally averaged marine surface data (both obtained from https://www.esrl.noaa.gov/gmd/ccgg/trends/gr.html). As shown in Fig. A2, the uncertainty of the satellite data is similar (mean value: 0.34 ppm/year) as the difference between the two NOAA time series (standard deviation: 0.21 ppm/year). We acknowledge that the maximum difference between any two latitude bands may be somewhat larger than the difference between the two NOAA time series shown in Fig. A2, but it is assumed that the difference shown in Fig. A2 is at least a reasonable approximation.

The agreement shown in Fig. A1 is interpreted as an indication of the good quality of the satellite XCO_2 data product and of the adequacy of the method used to compute the annual mean CO_2 growth rates because we do not find “strange values” in certain latitude bands or certain years, which would be an indication for a potential problem.

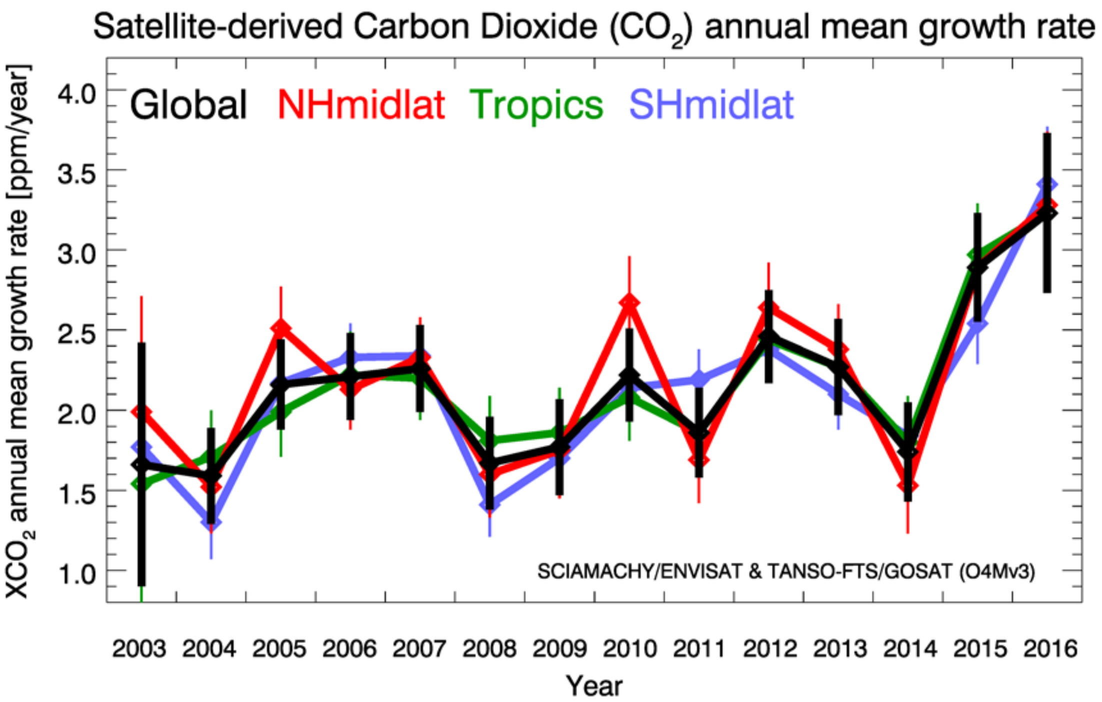

Figure A1. Satellite-derived annual mean XCO_2 growth rates: Global (black), Northern Hemisphere (NH) mid latitudes ("NHmidlat" (30°N - 60°N), red), Tropics (30°S - 30°N, green), and Southern Hemisphere mid latitudes ("SHmidlat" (60°S - 30°S), blue). The corresponding numerical values are listed in Tab. A1.

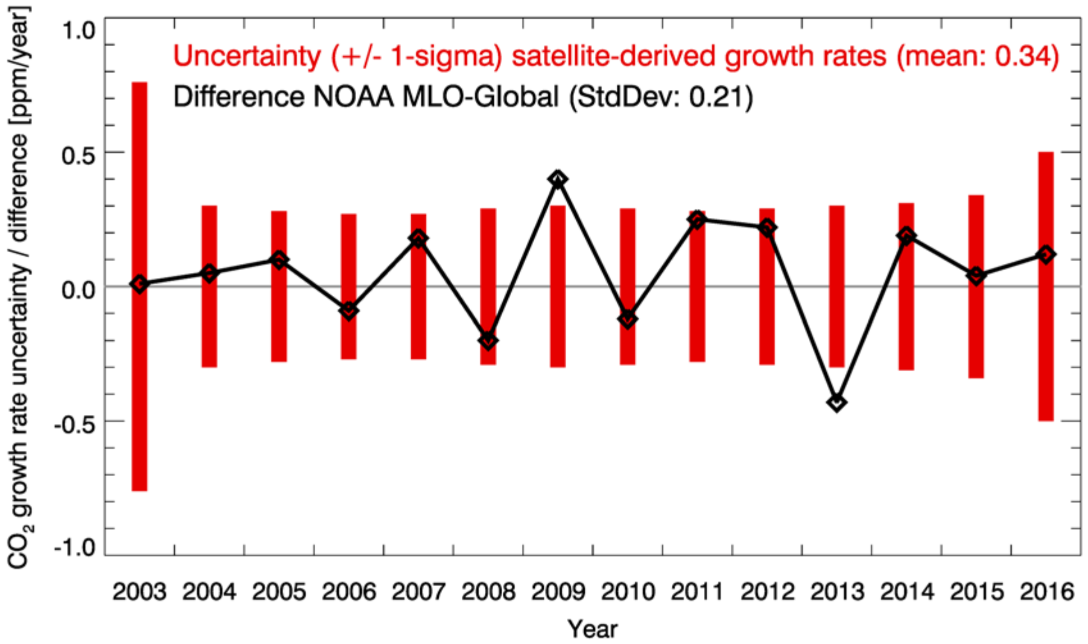

Figure A2. Comparison of the 1-sigma uncertainty range of the satellite-derived growth rates (red bars) with the difference of two annual mean growth rate time series obtained from NOAA, namely the time series from Mauna Loa (MLO), Hawaii, and the global time series obtained from globally averaged marine surface data (black line and symbols).

Table ~~2~~A1. Satellite-derived annual mean XCO_2 growth rates in ppm/year including 1-sigma uncertainty (in brackets). Abbreviations: NH is Northern Hemisphere and SH is Southern Hemisphere.

Year	Latitude band / region			
	Global	NH mid-latitudes (30°N-60°N)	Tropics (30°S-30°N)	SH mid-latitudes (60°S-30°S)
2003	1.66 (0.76)	1.99 (0.72)	1.54 (0.74)	1.77 (0.62)
2004	1.59 (0.30)	1.52 (0.29)	1.71 (0.29)	1.30 (0.23)
2005	2.16 (0.28)	2.51 (0.26)	1.99 (0.28)	2.17 (0.22)
2006	2.21 (0.27)	2.13 (0.25)	2.22 (0.27)	2.33 (0.21)
2007	2.26 (0.27)	2.33 (0.25)	2.20 (0.26)	2.34 (0.21)
2008	1.67 (0.29)	1.60 (0.27)	1.81 (0.28)	1.41 (0.20)
2009	1.77 (0.30)	1.75 (0.30)	1.86 (0.28)	1.70 (0.21)
2010	2.22 (0.29)	2.67 (0.29)	2.08 (0.27)	2.14 (0.20)
2011	1.86 (0.28)	1.69 (0.27)	1.86 (0.27)	2.19 (0.19)
2012	2.46 (0.29)	2.64 (0.28)	2.44 (0.27)	2.38 (0.21)
2013	2.27 (0.30)	2.38 (0.28)	2.27 (0.28)	2.10 (0.22)
2014	1.74 (0.31)	1.53 (0.30)	1.80 (0.29)	1.84 (0.23)
2015	2.89 (0.34)	2.89 (0.31)	2.97 (0.32)	2.54 (0.25)
2016	3.23 (0.50)	3.28 (0.46)	3.23 (0.48)	3.41 (0.36)